Uncertainty analysis of Hydraulic Boundary Conditions of the Wadden Sea

Phase 1 of Activity 2.3 of SBW Waddensea

Activity 3.2 of SBW project Waddenzee

Report

July 2007

H4918.31

Uncertainty analysis of Hydraulic Boundary Conditions of the Wadden Sea

Phase 1 of Activity 2.3 of SBW Waddensea

Joost Beckers, Neelke Doorn, Hanneke van der Klis

Report

July 2007

Contents

1 Introduction

1.1 Background

This report is the next step in the uncertainty analysis of the Hydraulic Boundary Conditions (HBC) calculations. This effort was started in 2006 with a predominantly qualitative inventory of expert opinions (WL, 2007a). By the end of 2007, we aim to give a more quantitative and comprehensive overview of the uncertainties in the results of the Wadden Sea HBC calculations. This report gives a specification of how the uncertainty analysis will be done and which sources of uncertainty will be investigated. Since the wave model SWAN is an important part of the HBC calculations, this model receives special attention.

The goal of the uncertainty analyses within the SBW Wadden Sea project is to find out which accuracy in HBC can be achieved, given the current state of scientific knowledge and technical instruments. Furthermore, we wish to quantify the contribution of the SWAN model and other components to the overall uncertainty in HBC.

In order to answer these and related questions we first need to identify and quantify all the possible sources of uncertainty in the HBC calculation. This report gives an overview of the sources of uncertainty that contribute to the overall uncertainty of the HBC in the Wadden Sea. Most of the uncertainties can only be quantified roughly, for example by an estimate of the bandwidth or variance. For the present study this is sufficient. The next step is to analyse how the sources of uncertainty propagate in the resulting HBCs. This report gives a specification of the calculations that are expected to give insight in the error propagation of the relevant sources of uncertainty. The calculations themselves will be done in the second half of 2007 and the results will be reported in a follow-up document.

1.2 Project plan

A number of activities were mentioned in the proposal[1] and the project plan. Below, we list these activities and refer to the sections in this report where the results are discussed.

Part 1A: Specification of the SWAN uncertainty analysis.

- Selection of a relevant SWAN area schematization.
  See Section 3.3.

- Specification of the SWAN uncertainty analysis: which processes are switched on or off, what is the probability distribution of uncertain parameters, boundary conditions, bathemetry, etc.
  See Section 3.2.

[1]Uitvoering Plan van Aanpak SBW RVW Waddenzee 2007, versie maart 2007.

- Development and testing of SWAN in the UATools environment, using the SWAN version delivered by HKV Lijn in Water.
  This activity will start after the delivery of the SWAN version by HKV, which is scheduled for July 2007.

- Reporting the findings of the activities mentioned above, including a possible adjustment of the plans for the SWAN uncertainty analysis.
  See this report. Based on discussions with Jacco Groeneweg and Ferdinand Diermanse we have no reason to adjust the original plans for SWAN uncertainty analysis. We do not foresee any insurmountable objections against the required calculations for the Wadden Sea area.

Part 1B: Specification uncertainty analysis of the HBC chain

- Identification of all sources of uncertainty in the HBC chain, using available literature, expert opinions and measurement data.
  See Section 2.1.

- Specification of the method to analyse the propagation of the various uncertainties through the HBC chain and how this affects the uncertainty in crest level.
  See Section 2.2 and Chapter 4.

- Founded choice of the relevant test locations and dike properties.
  Dike properties are specified in Section 2.2.11. Three locations are proposed in Section 4.5.

- Inventory of the adjustments to the Hydra-K software, necessary to calculate HBC for the Wadden Sea.
  This has been discussed with Ferdinand Diermanse. If the Matlab version of Hydra-K can be used, we do not expect any problems. However, it will take a few days work (6 days, activity 1c of Phase 2) to adjust and test the software.

- Specification of the SWAN calculations that form the base of the KustDB for the selected test locations.
  See Section 2.2.8. The size of the database (hence the number of SWAN calculations) will be kept as small as possible. Therefore, we will consider only 5 wind sectors (mainly North wind), 4 water levels and 7 wind speeds. This amounts to a total of 140 SWAN calculations. The actual SWAN calculations and the build-up of the database in phase 2 will require an estimated 11 days in total.

- Choices for any approximations or proxies that will be used for missing data.
  See Chapter 4.

Finally, at the moment of writing the project plan and proposal it was not yet clear whether it was possible to distiguish between the various contributions to the total uncertainty in HBC.

In Chapter 4, we propose a method that will quantify the relative contributions from the two main sources of uncertainty.

1.3 Outline

The outline of the report is as follows:

- In the following Sections 1.4 and 1.5 we give a general overview of the HBC calculations and a summary of the uncertainty analysis, which has been done in 2006.
- Chapter 2 gives a detailed description of the steps of the HBC calculations and an analysis of the various sources of error and uncertainty.
- Chapter 3 deals with the sources of uncertainty in SWAN, which is an important part of the HBC calculation.
- Finally, Chapter 4 describes the approach to combine all relevant sources of uncertainty in an overall uncertainty analysis.

The actual quantitative uncertainty analysis will be done during the second half of 2007.

1.4 General description of the model chain

The method to determine the Hydraulic Boundary Conditions (HBC) consists of several components, which can be described as a model chain. In this chapter we describe the general model chain, as far as necessary to understand the following chapters. For a detailed description we refer to Den Heijer *et al* (2006).

Figure 1 shows the model chain used to compute the HBC along the Dutch coast. Although this chain has not yet been used for the Wadden Sea, this is expected to happen for the computations of the HBCs of 2011.

The central model in this chain is *Hydra-K*. Hydra-K represents a probabilistic method to compute the HBC at locations along the coast that represent the hydraulic load used for the design of sea defences. The probabilistic method is based on a Monte-Carlo technique, with the assumption that the correlation between different factors under extreme conditions correspond with measured correlations (the so-called method ‘De Haan’). Hydra-K computes the hydraulic design conditions for different failure mechanisms, such as wave run-up, or damage of the dike revetment. The hydraulic design conditions differ between failure mechanisms, because different parameters determine the moment of failure of the dike.

We note that other Hydra-models exist to compute the HBCs for other water systems in The Netherlands: Hydra-B (western part of the river system of Rhine and Meuse), Hydra-M (lakes) and Hydra-VIJ (delta of rivers Vecht and IJssel). All Hydra-models are based on a probabilistic computation method (TAW1998, HR2001).

In contrast to the HBC computation for the Dutch coast, the Wadden Sea HBC will only consider water level and wind (speed and direction) at deep water as random input variables. Analogously to the Oosterschelde area, the wave height and wave period are considered fully correlated with the wind speed.

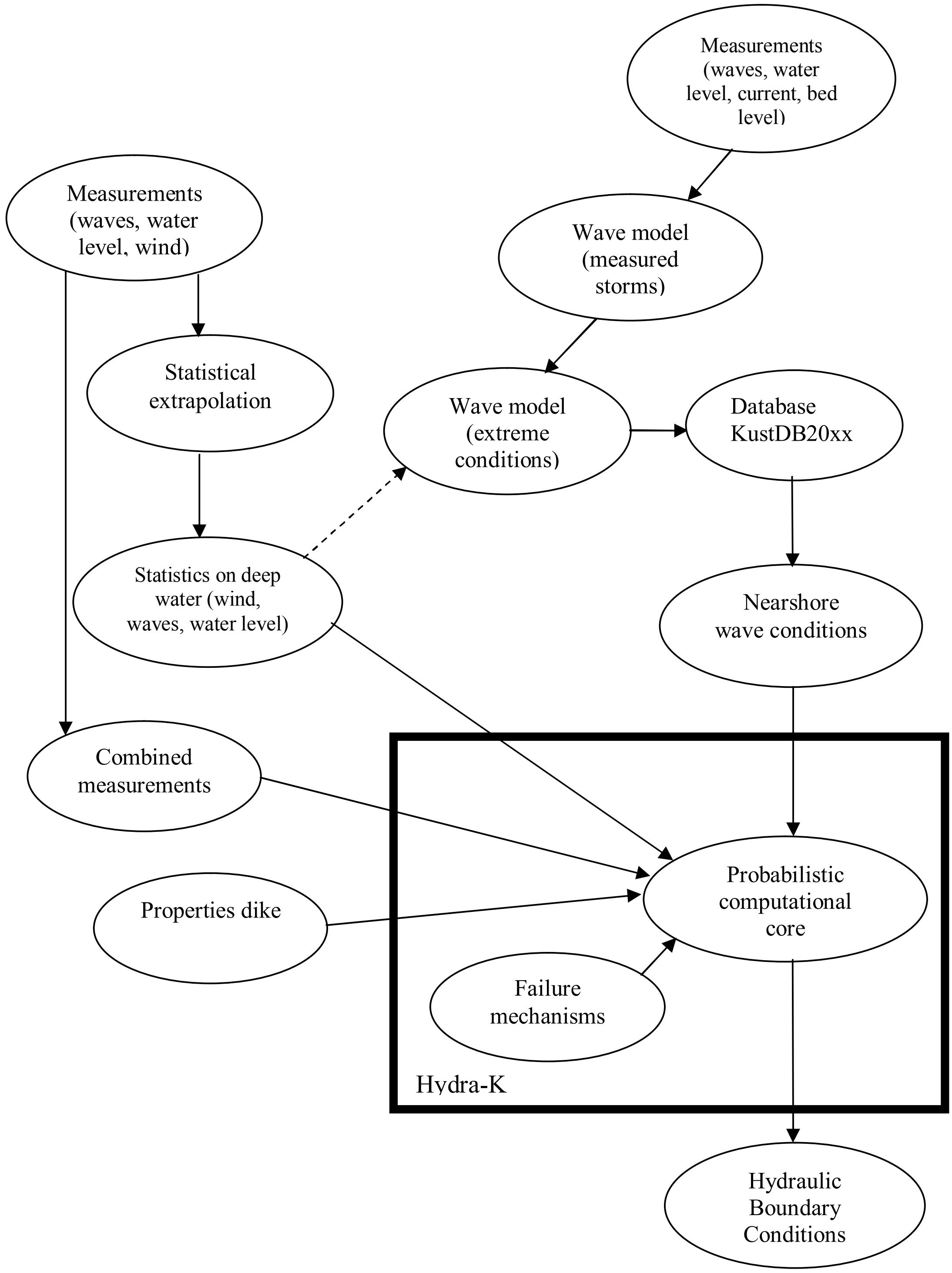

Figure 1: Model chain for the computation of HBCs in the Wadden Sea.

This model chain results in HBCs for a given failure mechanism at a given location. Examples of HBCs (the so-called illustration points) are published every five years by the Ministry of Public Works, Transport and Water Management, i.e. water levels and waves characteristics for specific return periods. Changes in HBCs indicate changes in (our knowledge of) the water systems. Actual changes in safety levels of flood defences are determined by water managers using Hydra-K on true dike cross-sections. Hydra-K is a mandatory tool for assessing dike heights and dike strength.

Hydra-K uses the probabilistic computation method known as the method of 'De Haan' (De Haan and Resnick, 1977). The basis of this method is a set of measurements of water levels, wind and (optionally) offshore wave parameters (at approximately 20 m water depth). In the example of Figure 2 these parameters are represented by the cloud of black dots in the lower left corner. Each dot represents the maximum value of the water level in a single storm event, and the corresponding wind speed.

The method of 'De Haan' assumes that the correlation between water level and wind speed for the observed storm events is be the same for extreme events (so-called asymptotic dependency). This means that we can define a set of extreme events by translation of the observed events as shown in Figure 2. The purpose of this translation is to obtain a sub-set of (synthetic) events that lead to failure of the dike. In Figure 2 these failure events are represented by the open circles to the upper right of the bold line.

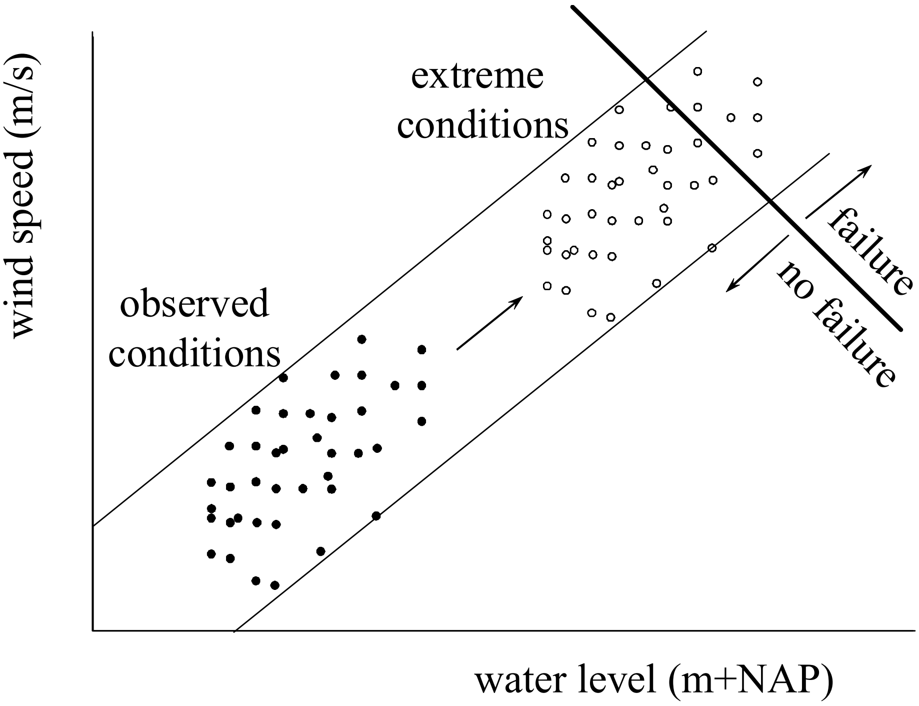

Figure 2 Schematic view of up-scaling storm events in the method "De Haan".

The translation follows the line of 45° in the *exponential space*, which represents the probability of exceedance of both variables. The translation along the line of 45° in the exponential space corresponds to a multiplication of the respective probabilities of exceedance of the observed water level and wind speed by the same factor. If we consider an observed pair of offshore water level and wind speed (h, U_w) with individual probabilities of exceedance (P_h, P_U), then the translated, or up-scaled, pair (h*, U_w*) will have a probability of exceedance of (cP_h, cP_U), where: $0<c<1$. So if c equals 10^{-3} a 'regular' storm event with an exceedance rate of 0.1 per year then becomes an extremely unlikely event with exceedance rate $0.1*10^{-3} = 10^{-4}$ per year.

Hydra-K determines the offshore water level and wind speed (h^*, U_w^*) of the up-scaled storm event using the individual probability distribution functions (see Figure 21). In the example above, Hydra-K applies the inverse of the probability distribution function of water level to determine the water level with an annual probability of exceedance equal to 10^{-4}.

The failure rate of the dike in Hydra-K is determined as follows:

$$\mu = \frac{\kappa}{\Delta} e^{-\upsilon} \tag{1.1}$$

with:

μ = annual failure rate of the dike;
κ = number of up-scaled storm events that lead to failure;
υ = measure for the length of the translation;
Δ = length of the time series of observed events in years.

Hydra-K can compute a critical crest level of a dike corresponding to a given failure rate. In the Netherlands, dikes along the coast are designed for safety levels of the order of 10^{-3} to 10^{-4} 'failures' per year. This frequency is based on both the economic value of the protected area and the extent of the threat. For the purpose of design we can rewrite Equation (1.1) as follows:

$$\upsilon = -\ln\left(\frac{\mu \Delta}{\kappa}\right) \tag{1.2}$$

All parameters on the right-hand side of Equation 2.2 are known. The standard failure rate of a dike in the Wadden Sea area is μ=2.5*10^{-4} annually, or once per 4000 years. The length of the observation period of storm events, Δ, is 24 years. The number of failure events, κ, is a user defined number (default: 50). The translation length, υ, then follows from (1.2). For κ=50, we obtain υ=9.03.

The observed storm events are translated according to the value of the translation length, υ. Subsequently, Hydra-K computes the nearshore wave parameters and water levels that result from the up-scaled offshore water levels and wind speeds. For this purpose Hydra-K uses the wave simulation model SWAN (or actually, a database with SWAN computation results). In this way, for each up-scaled storm event the nearshore hydraulic load, consisting of water levels, wave heights, wave periods and wave directions, is considered. The nearshore hydraulic load is compared with the resistance of the dike to find out for which up-scaled storm events the dike is expected to fail. For this purpose a so-called 'reliability function' has been implemented for each relevant failure mechanism in Hydra-K, in accordance with (VTV, 2004).

Given a failure rate, μ, the critical crest level is derived iteratively in such a way that exactly κ events lead to failure. The resulting dimensions then exactly fulfil the stated safety norm.

1.4.1 Additional random offshore variables

The method as described in the previous sections only considers wind (speed and direction) and water level as random variables. All other variables such as offshore and nearshore wave parameters are derived from wind and water-level, based on deterministic relations. However, there is no limit in the method of 'De Haan' to the number of random variables, as long as the assumption of asymptotic correlation holds for all these random variables. In 2006 an additional random variable for the Dutch coast (Hollandse kust) has been implemented in Hydra-K: the spectral wave period $T_{m-1,0}$. This feature is optional in Hydra-K, i.e. the user can choose whether $T_{m-1,0}$ is considered as a random variable or still deterministically related to wind and water level. For the Wadden Sea HBC this additional random variable has not been used for reasons that will be addressed later.

1.5 Uncertainty analysis

1.5.1 General

Uncertainty is defined as the discrepancy between a calculated value and its 'true' value. The problem is, of course, that we do not know the true HBC. Still, we can make an estimate of the errors that are inevitably associated with the steps in the calculation process. This estimation of the possible discrepancy takes into account both random errors and bias, or systematic errors.

1.5.2 Uncertainty expressed in crest level

The HBC are usually represented by a so-called illustration point: one combination of water level and wave conditions from the collection of all possible hydraulic loads that combined have the designated exceedance probability. An illustration point for a sea defence consists of four parameters:

- water level at the toe of the sea defence
- nearshore wave height
- nearshore spectral wave period
- wave incident angle

The uncertainty in the HBC calculation manifests itself as an uncertainty in each of these four parameters. However, the various sources of uncertainty in the HBC calculations contribute differently to the four parameters. For example, the uncertainties in the SWAN model only affect the wave parameters, not the water level. This complicates the prioritization of efforts to minimize the overall uncertainty.

Another way to represent the HBC is to compute the minimally required crest level of a virtual dike (design dike) that would withstand the HBC at the location of interest. For this we assume that the failure mechanism 'wave overtopping' is dominant and consider a dike with a fixed slope that can be extended indefinitely. The critical crest level is then a single scalar quantity that is associated with a given set of HBC. Consequently, the uncertainty in the HBC is also expressed as a single scalar. This is very convenient because the contributions to the total uncertainty in the crest height can now be determined unambiguously. It is also clear what reduction in the total uncertainty can be expected by minimizing one of the sources of uncertainty (Den Heijer *et al*, 2006).

1.5.3 Results of the 2006 study

From the inventory of expert opinions (WL, 2007a) a list of most important sources of uncertainty in the HBC for the Wadden Sea has been derived:

1. The *inherent* uncertainties concerning the extrapolation of meteorological and offshore hydraulic conditions to extremely large return periods (of the order of 10^3 up to 10^4 years). This large uncertainty directly affects the HBC computed by Hydra-K, from the point of view of the legal safety standard of the sea defences. In other words, due to this inherent uncertainty it is unclear whether the computed design dike dimensions are sufficient to fulfil the legal safety standards.

2. Given the offshore conditions, it is the *model* uncertainty of the SWAN model and its input parameters that lead to an uncertainty in the nearshore HBC. The major contributions are:
   - The suitability of SWAN for extreme conditions, in particular because of the uncertainties concerning the model formulations. That is to say, the uncertainty in parameterization of physical processes, such as triads, white-capping and surf-beat, in particular those affecting the nearshore wave *period*.
   - The uncertainties in the derivation of the wind field used by SWAN and the modelling of the interaction between wind and waves, especially for strong wind.
   - The uncertainty in the bed topography of the Wadden Sea, in particular near the sea defences, affecting the nearshore wave *height*.
   - The lack of measurements of currents in the Wadden Sea, combined with the lack of knowledge of the effect of currents on the nearshore HBCs.

From the quantitative sensitivity analysis performed for three locations along the Dutch coast we conclude the following (WL, 2007a):

1. The effect of the uncertainty in the offshore water level, wave characteristics and wind and in the nearshore wave characteristics on the uncertainty about the design crest levels is substantial. Quantified, the uncertainty in the crest levels due to these uncertain parameters is of the order of meters, which is considerable in terms of dike design.
2. Of the parameters taken into account, the design crest level is most affected by the uncertainty in the wave periods, both nearshore and offshore. Note that the computations in which the *offshore* wave period has been varied are less reliable.
3. The effect of uncertainty in each of the varied parameters is highly depended on the location along the coast.

The overall uncertainty in the HBC at a single location is determined by several local conditions, such as the influence of offshore waves and the influence of currents. This implies that the uncertainty varies per location. Roughly speaking, it seems that the HBCs of the western part of the Wadden Sea are less sensitive to uncertainties than those in the eastern part. In the eastern part the uncertainty with respect to the penetration of long waves hitting the sea defences is important.

2 Quantitative uncertainty analysis of HBC

2.1 Introduction

Figure 3 shows the model chain used to compute the HBCs along the Dutch coast. Figure 3 is a more detailed version of Figure 1, focussing on the data flow. Every step in the calculation introduces some type of uncertainty. All uncertainties combined lead to an uncertainty in the HBCs, which is represented by the critical crest level in this study.

In this chapter, we address each step and discuss the possible sources of uncertainty. In principle, all uncertainties propagate to an uncertainty in the end result. However, some contributions are negligible compared to others (indicated in green in Figure 3). Other sources will be investigated in detail in other projects (indicated in yellow in Figure 3). All the remaining relevant uncertainties (indicated in red in Figure 3) will be quantified in this report and their propagation to the end result will be analyzed in phase 2 of the SBW project, in the second half of 2007.

Similar to wind and water level, wave height and wave period are input variables of the SWAN model and as such influencing variables on the nearshore wave conditions. In the Hydra-K version used for this study, the offshore wave height and period are assumed to be fully correlated to the wind speed. H_{m0}, and $T_{m-1,0}$ are computed deterministically from U_w. The variation in the offshore wave height is considered to have only minor effects on the nearshore wave conditions, since the shallow Dutch shores cause high waves to break before they reach the dike system.

However, the method 'De Haan' sets no limits to include wave parameters as random variables, such as the offshore significant wave height, H_{m0}, and offshore wave period $T_{m-1,0}$. In future versions of Hydra-K the parameters H_{m0} and $T_{m-1,0}$ might therefore be added as additional random variables. The addition of H_{m0} as a random parameter is expected to show only marginal effects. The variation of the offshore wave period may have a larger impact. For the moment, this parameter is still assumed fully correlated to the wind speed, because in earlier work the inclusion of the offshore wave period as a stochastic variable led to unreliable results (WL, 2007a).

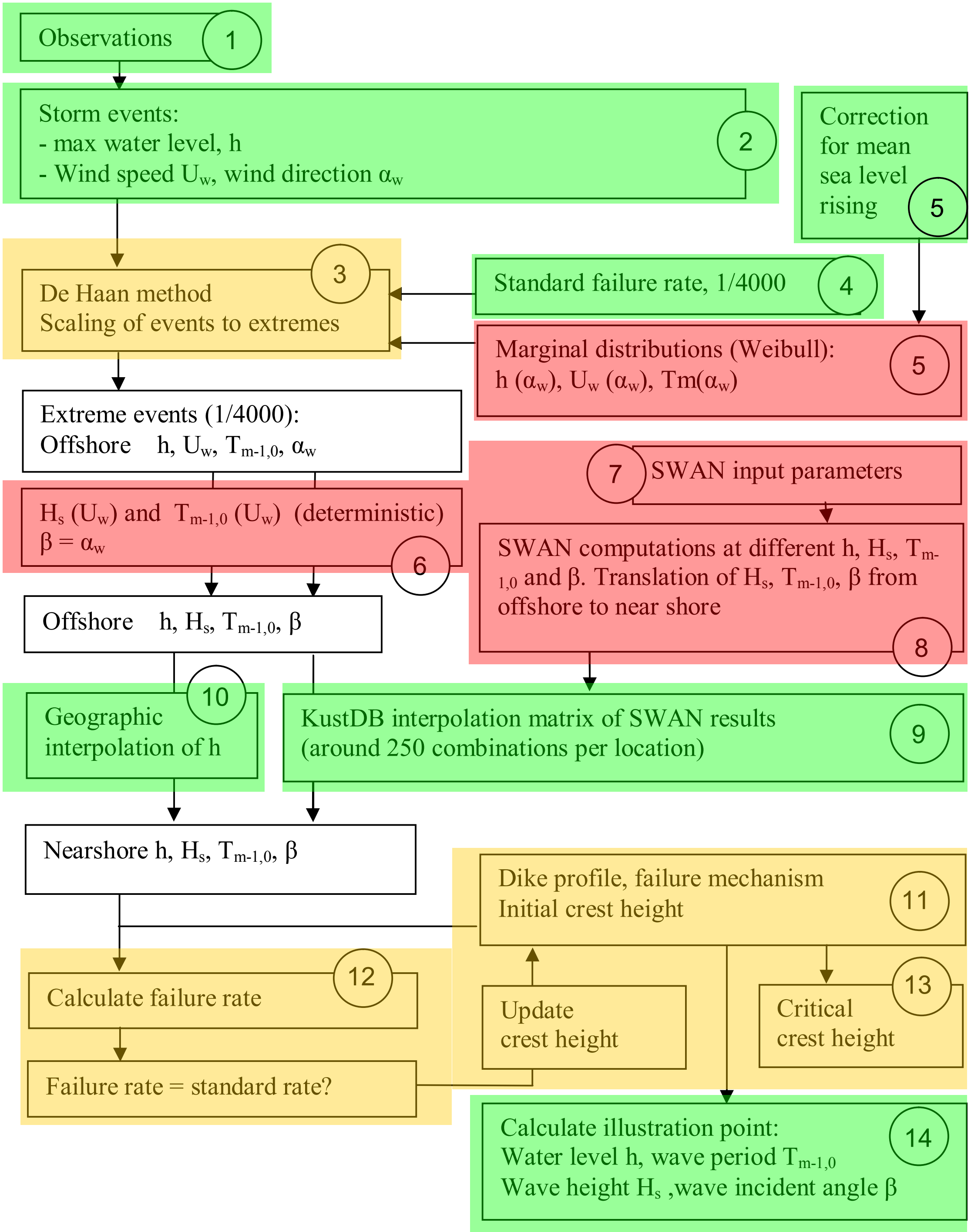

Figure 3: Schematic overview of the HBC calculation.

Green: These sources of uncertainty are negligible as will be shown in the next sections.

Red: These sources are dominant and will be quantified in detail in the following sections.

Yellow: These sources will be investigated in other projects, in the second half of 2007: The 'De Haan' method (3) is investigated by WL | Delft Hydraulics outside the SBW framework. The failure calculations (11-13) are investigated by GeoDelft within the SBW framework ('onzekerheidsanalyse faalmechanismen').

2.2 Quantification of uncertainties

2.2.1 Observations (no. 1 in Figure 3)

Observations of water levels and wind are used for three purposes in the HBC calculation. First, the probability of exceedance curves for wind speed and water level (step 5) are based on observations that originate from many sources with varying quality. Secondly, the deterministic relations between wind speed and wave parameters (step 6) are based on simultaneous observations. Thirdly, Hydra-K uses observations to define storm events that are up-scaled in the 'de Haan' method (step 3). In the following, we consider the uncertainty in the observations of water levels, wind and waves.

In general, measurement uncertainty consist of inherent and statistical uncertainty. The inherent uncertainty results from natural variability in space and time and cannot be reduced. The statistical noise in the measurements, however, can be reduced by averaging over a longer period.

Water level

The sea-water level is sampled by using floats at several monitoring stations along the Dutch coast. A digital level sampler (Dutch: Digitale Niveaumeter, DNM) takes samples approximately every second. A microprocessor averages the collected samples every 10 seconds and sends the result to a central computer. This computer calculates the 10 minute average and stores it in a database (DONAR). The reference for the water level is the Normaal Amsterdams Peil (NAP).

The observed water level signal suffers from noise, caused by (long) waves. The 10 minute averaging reduces this statistical error to approximately 2 cm (estimated from Figure 4). There is also a possibility of a systematic error in the observation, for example due to errors in the measuring equipment. Since the equipment is regularly calibrated and checked for consistency with other stations, we do not expect this bias to exceed a few centimeters.

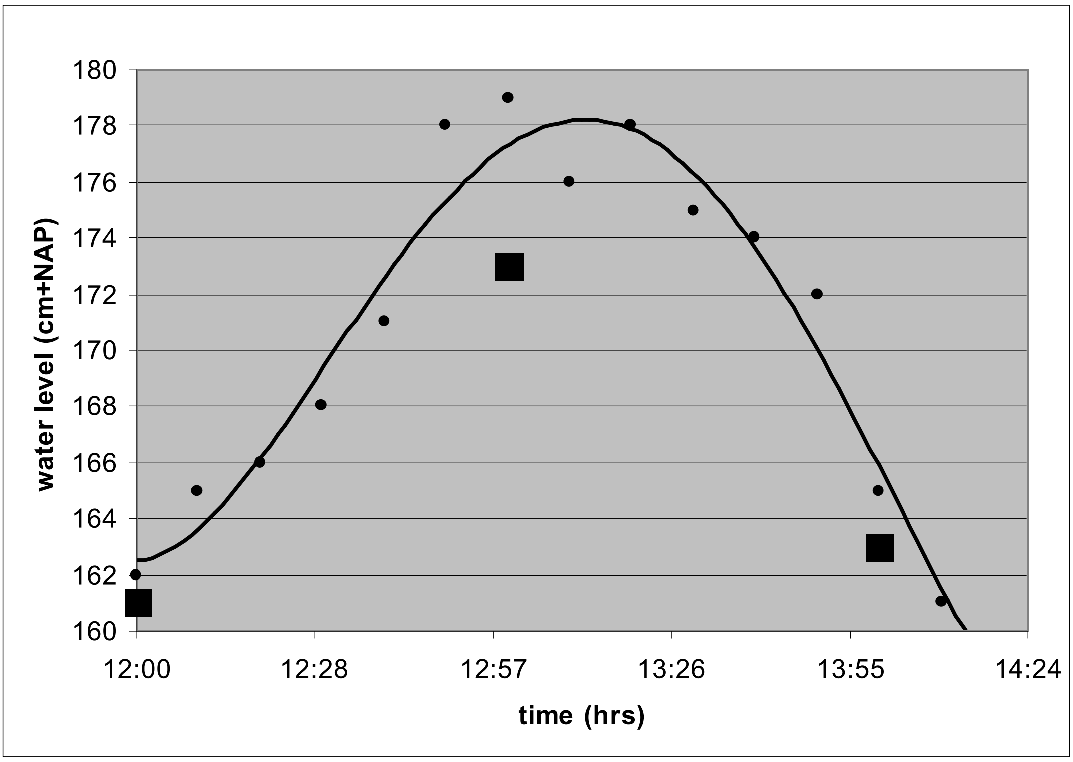

Figure 4: Water level during a storm surge at Harlingen. Small circles are 10 minute observations, large squares are 1 hour averages. The curve is an indicative fit and gives an impression of the measurement error.

Hydra-K uses one hour averages (see Figure 4) and an additional 'moving average' filter (den Heijer *et al*, 2006) to reduce statistical noise as much as possible, while still capturing the peak of the storm. The total uncertainty in the maximum observed water level, with several contributions, is estimated at 5 cm at most (standard deviation).

Wind

Wind speed, wind direction and other meteorological parameters are monitored at about 50 locations in the Netherlands by KNMI. The wind measurements are influenced by the local environment of the measurement site, which is expressed in a 'roughness length'. From this roughness length the wind speed at a reference level (a height of 60 m) is computed using a logarithmic wind profile. This 60-m wind is in turn used to compute the wind over a hypothetical measuring site. When for this hypothetical site a measuring height of 10 m is used, and a roughness length 0.03 m (WMO requirements), the resulting wind speed is called the 'potential wind' speed.

This potential wind at the Dutch measuring stations is stored every hour and published online. The potential wind speed is reported in 0.1 m/s, but the resolution of the records from which it was computed is approximately 0.5 m/s. From July 1996, wind speed is measured in integer values of m/s. So since then the resolution is even less (Verkaik, 2001).

KNMI publishes 10 minute averages and 1 hour averages of wind speed and direction. Hydra-K uses the 1 hour averages. The uncertainty in the observed wind speed is estimated by (Verkaik, 2001) as 10% (standard deviation). The uncertainty in wind direction is 5º.

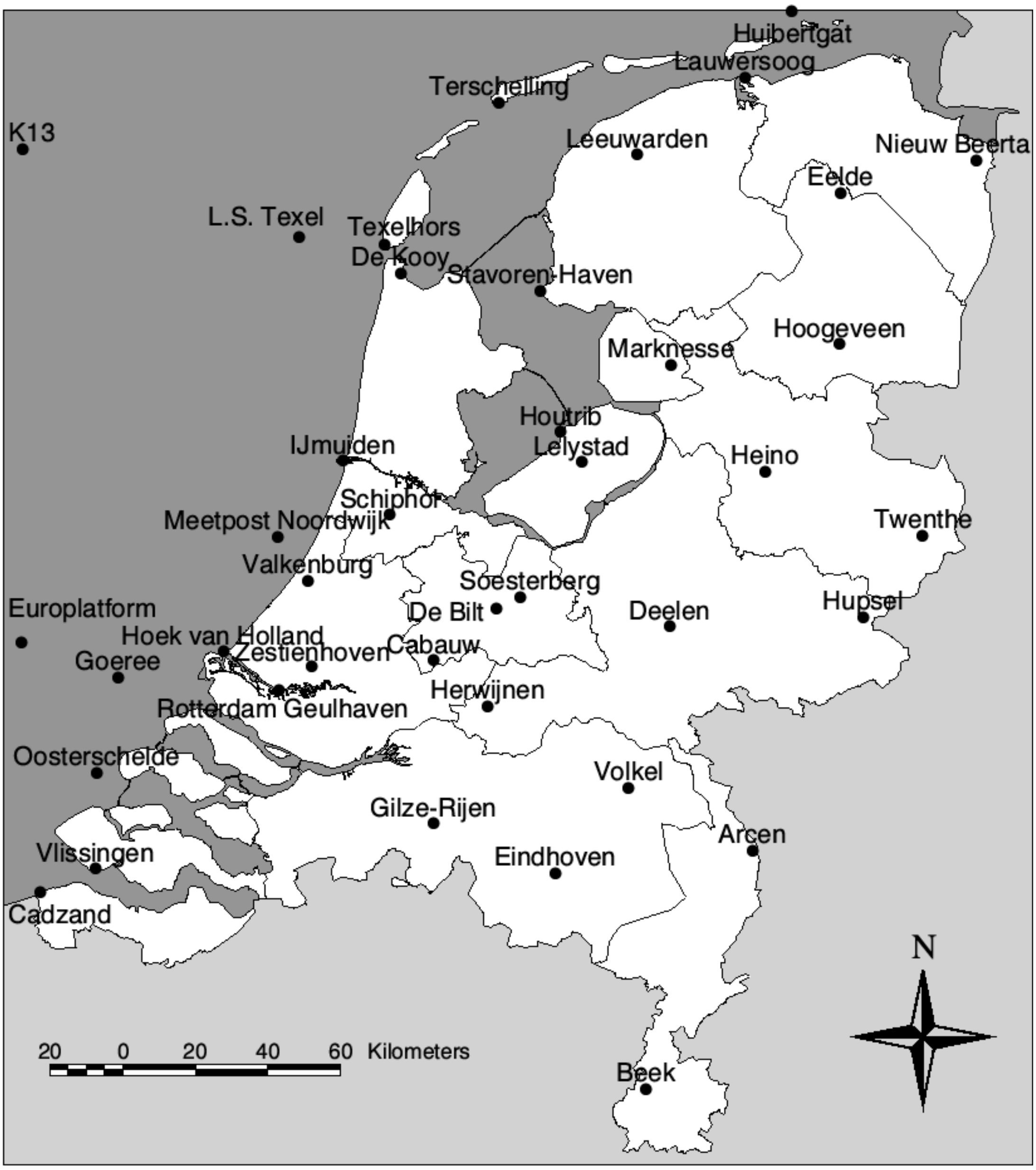

Figure 5: Wind measurement stations in the Netherlands.

Wave measurements

Wave height, direction and period are measured by directional Waverider buoys that are part of the North Sea measuring network (Dutch: Meetnet Noordzee) maintained by RWS Directie Noordzee. The four main buoys are EUR, IJM, ELD and SON (see Figure 6). They are situated at relatively deep water beyond the influence of dynamical processes in the nearshore waters (e.g. sandbanks) that could disturb the long term statistics.

The Waverider buoy follows the dynamics of the water surface and records the vertical accelerations. Using a compass as a reference the buoy can derive the height, direction and period of the passing waves. The measurements are averaged over 10 minute periods, digitized, and send to a central database (DONAR) by radio. DONAR averages the received data over 1 hour periods.

The default parameters that are stored in DONAR are:

- The significant wave height (Hm0);
- The average wave period (Tm02);
- The mean direction of the passing waves (Th0);
- The average spread in the direction of the waves (SObh);
- The significant height of the low frequency waves (HTE3);
- The direction of the low frequency waves (Th3);
- The average height of the highest 1/3 of the waves (H1/3);
- The average period of the highest 1/3 of the waves (TH1/3).

The measurement error in the wave height parameters is estimated at 5% in deep waters and 10-15% in shallow waters (WL, 2007a and Den Heijer *et al*, 2006). The uncertainty in the wave period is about 2.5% (all standard deviations). These uncertainties propagate in the SWAN calculations, see Chapter 3.

2.2.2 Storm events (no. 2 in Figure 3)

Hydra-K is based on the ‘de Haan’ method of up-scaling of observed storm events (see step 3). These storm events are selected from water-level time series at a number of water-level monitoring stations along the Dutch coast (triangles in Figure 6). In the Hydra-K version used for this study, the storm event is defined by the maximum offshore water level and the corresponding wind. Any stronger wind just before or after the peak of the water level is disregarded. For the failure mechanism ‘wave overtopping’ this is probably correct, i.e. the largest overflow occurs around the maximum waterlevel. For other failure mechanisms the highest load may occur at a different moment, when the water level is not at its maximum. Failure of the dike revetment, for instance, will probably occur at the point where the wave impacts are strongest, which not necessarily coincides with the highest water level. If this is taken into account, some computational difficulties occur, since the failure domain is not regular anymore. In these cases, the implemented computation method does not identify the illustration point correctly (personal communication F. Diermanse). This problem will be further investigated in a project outside the framework of SBW, scheduled for the second half of 2007 (Validatie ‘De Haan’).

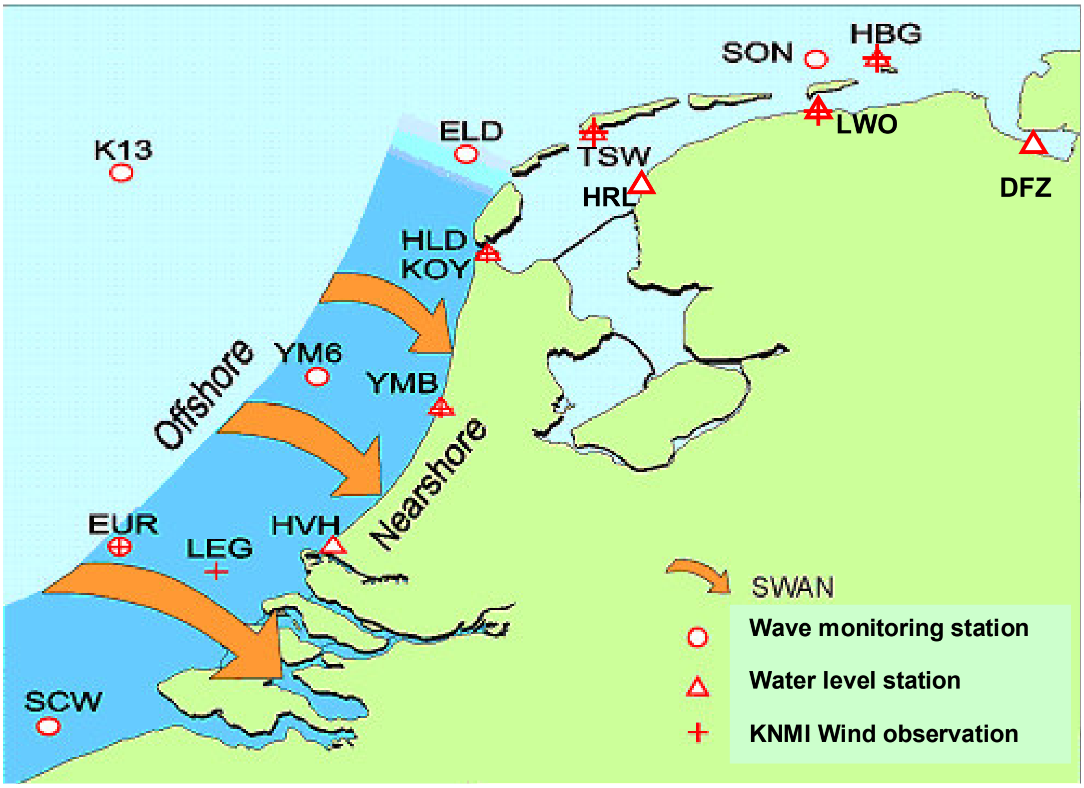

Figure 6: Water level, wave and wind monitoring stations.

The wind speed is taken from one of the nearby KNMI wind observation stations at the time of the maximum water level. The water level and wind monitoring stations can be at different locations, but the error introduced by the difference in time of the peak of the storm is considered negligible. This is based on comparison with other errors and considering the fact that all the observation data are hourly averages.

The wind speed at the wind monitoring stations is transformed into a 'potential wind' speed (see step 1). This wind is used in determining the offshore wave height (step 6) as well as the wind field input in SWAN (step 7). The wind input for SWAN is based on the 'open water wind', which is derived from the potential wind by an 'open water transformation'[2].

For more information about the selection of storms we refer to Van Marle (1999) and Groenewoud and De Valk (1999).

2.2.3 De Haan sampling method (no. 3 in Figure 3)

Hydra-K uses the so-called method 'De Haan', with the basic assumption that the correlation between offshore wind speed and water level under normal conditions is the same as under extreme conditions. This is called asymptotic dependence (AD).

[2] http://www.knmi.nl/klimatologie/onderzoeksgegevens/potentiele_wind/explanation.html

According to some experts, the assumption of AD can probably not be supported (Vrijling in WL, 2007a). Others (Diermanse in WL, 2007a) expect that this assumption does not influence the resulting design conditions very much, that is, in case of the failure mechanism of wave overtopping. From a study within the framework of the UBW project (Uniformering Belastingmodellen Waterkeren) it appeared that the difference in design conditions between the method 'De Haan' and other methods was relatively small (Ferdinand Diermanse, pers. comm.).

The 'De Haan' method has also been investigated in a study by Geerse *et al* (2006). The conclusion was that the validity of the method mainly depends on the quality of the probability of exceedance distributions of the offshore water level and wind speed. If these distributions are of poor quality, as in Voortman (2002), then the 'De Haan' up-scaling produces considerable errors. The uncertainty in the up-scaling method is therefore directly related to the uncertainty in the probability of exceedance distributions, which are addressed in step 5.

As part of the same study (Geerse *et al*, 2006), the influence of the 'De Haan' scaling factor, υ, and the number of events that lead to failure, κ, was investigated. The default number of failure events in Hydra-K is set to 50. According to Geerse this number is adequate and the results should not vary much for slightly different values. In fact, there is an option in Hydra-K to automatically find the optimal number of failure events (Stijnen *et al*, 2005). However, for failure mechanisms other than wave overtopping it has been observed that in some cases no optimal number of failure events could be found (e.g. failure of dike revetment).

The 'De Haan' method will be investigated further in a study that is scheduled for the second half of 2007. Therefore, we do not consider any uncertainty related to the 'De Haan' method in this uncertainty analysis.

2.2.4 Standard failure rate (no. 4 in Figure 3)

The standard (default) failure rate is defined by law (Wet op de Waterkering, 1995). For a dike along the Wadden Sea coast, the standard failure rate is $2.5*10^{-4}$ or 1/4000 per year.

The standard failure rates were set by the Delta Commission in the 1960's, based on economic Cost-Benefit analyses (Van Dantzig, 1956). One can argue that the economic situation has changed since then and that the failure rates should be recalculated. This is, however, far beyond the scope of the current project. We will assume that the standard failure rates are fixed.

2.2.5 Marginal distributions (no. 5 in Figure 3)

The water level and wind speed of the up-scaled storm events are derived from the probability of exceedance functions of the offshore water level and wind speed. These are derived from measurements at observation stations. Since the observation period is much shorter than the return period of the up-scaled events, there is considerable uncertainty in the statistical extrapolation of the measurements.

There are three possible sources of error in the marginal distributions:

- Measurement error (step 1). The curves are ’fitted’, using a formula that makes it possible to construct a smooth curve through the raw measurement data. The fitting reduces the statistical error because we take an average over many measurements.
- There is uncertainty about the shape of the curve, or the function that is used to fit the data (model uncertainty).
- Finally, we expect an error in the fitted parameters of the curve. Theoretically, this parameter uncertainty could be reduced by including more measurements. However, the possible observation period increases only slowly and will not exceed 100 years within our lifetime (statistical uncertainty).

The latter two types of error are responsible for most of the uncertainty in the lower-frequency tail of the curves, and it is this part of the curve that is used in the up-scaling. The error in the lower frequency part of the tail of the probability of exceedance distributions causes errors in the water level and wind speed of the up-scaled storm events.

In Hydra-K, both water level and wind speed are fitted to conditional Weibull functions. The general form of the conditional Weibull function is:

$$F(X > x) = \rho \exp\left\{ -\left(\frac{x}{\sigma}\right)^{\alpha} + \left(\frac{\omega}{\sigma}\right)^{\alpha} \right\} \qquad (2.1)$$

where:

F	= frequency of exceedance (1/year)
X,x	= quantity of interest (e.g. water level)
α	= shape parameter (-)
σ	= scale parameter
ω	= threshold, above which the distribution is valid
ρ	= exceedance rate of the threshold (1/year).

Wind speed

The wind observations from one or more monitoring stations around the Wadden Sea are fitted to conditional Weibull distribution functions and extrapolated to large return periods. The nearest stations for the Wadden Sea are de Kooy (KOY), Terschelling (TSW) and Huibertgat (HBG), see Figure 5 and Figure 6 for the geographical positions of these stations. In Hydra-K, the Weibull functions are not fitted to observations directly, but to data from the Rijkoort-Weibull (RW) model, which was proposed by Rijkoort (1983) for a large number of onshore locations in the Netherlands.

Rijkoort used observations from wind monitoring stations from 1962 to 1976. The observed wind speeds were converted to a potential wind speed (see step 1). Next, a two-piece (6 parameter) Weibull function is fitted to the data. A persistence correction is applied to change the return periods corresponding to single occurrences of wind-speed values to return periods corresponding with events of interest (storms). In Rijkoort (1983) the annual maxima are used to calculate this persistence correction. The onmi-directional exceedance rates are distributed over 12 wind sectors of 30º and for every wind sector a separate

Weibull function is constructed. The conditional Weibull distributions in Hydra-K that have been fitted to the high-wind tail of the RW model have the following parameters:

	YMS	TXL	TSW
ω (-)	22	24	23
ρ (1/year)	0.43	0.45	0.47
α (-)	1.93	2.16	2.09
σ (m/s)	9.69	12.1	11.31

The extrapolation of wind speed to extreme values with 4000 year return periods is associated with a number of uncertainties:

First, the extrapolation requires a fitting function to the observed data. There are alternatives to the fitting function used in the RW model that can lead to different results. As part of the Hydra project, KNMI (Verkaik, 2003; and Smits, 2001) constructed new models for extreme wind speeds. Instead of the hourly observations and the persistence correction, Verkaik used a peaks-over-threshold (POT) approach, with a 48 hour window around each peak. The data sets were fitted to a conditional Weibull distribution (CWD) and a generalized Pareto distribution (GPD). The advantage of the POT method is that the peaks are independent and no persistence correction is required. Unfortunately, the results for inland stations were inconsistent with those for stations along the coast, so the results were not usable for Hydra-K. Still, the results give an indication of the model uncertainty caused by the choice of a Weibull fitting function. Smits (2001) proposes a Generalized Extreme Value (GEV) model and a Markov chain model. Figure 7 shows the different fits. Based on Figure 7 we estimate that the model uncertainty, associated with the choice of the RW model, is at least 5 m/s (standard deviation) for return periods of 4000 years.

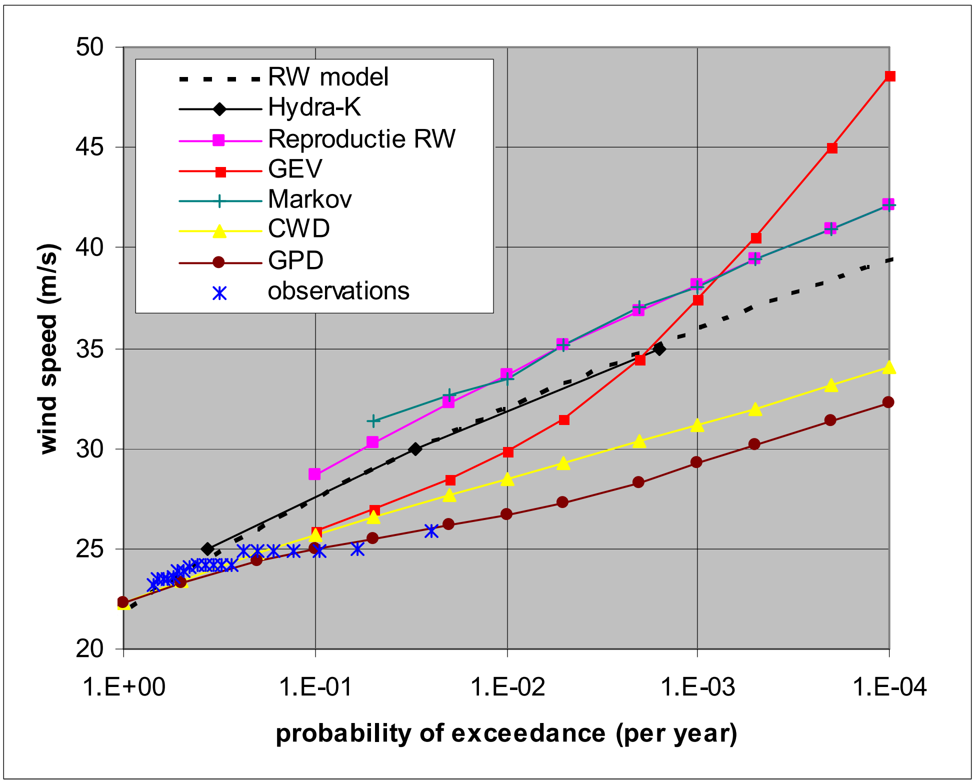

Figure 7: Different probability of exceedance models and observations of the wind speed at Texel.

Secondly, the observation period used for the RW model covered only 15 years (1962-1976). This causes significant statistical uncertainty in the parameters of the fitting function. KNMI (Smits, 2001) compared the RW model to a similar model fitted on observations from 1981 to 1995. The differences between the two fits gives an impression of the statistical uncertainty in the Weibull parameters. For example, the wind speed at Leeuwarden for a return period 1000 years from the original RW is 29.9 m/s, whereas the new fit produced 32.5 m/s. Averaging between the monitoring stations, the difference between the two fits for return periods of 1000 years was 3.5 m/s in wind speed. For return periods of 4000 years, this uncertainty is estimated at about 4 m/s by extrapolation. In order to reduce this uncertainty, it is possible to apply a Bayesian analysis. This is, however, not the subject of the current study.

The conditional Weibull fit to the RW data also results in minor errors at extreme wind speeds. For return periods in the range of 1000 to 10.000 years the differences are generally smaller than 0.1 m/s (Den Heijer *et al*, 2006), compare the solid black and dashed black lines in Figure 7. This difference is negligible compared to other uncertainties.

There is one additional assumption that causes uncertainty. The RW wind statistics that form the basis for the wind in Hydra-K provide the exceedance rate for wind speed during any storm, irrespective of water level. However, Hydra-K needs the exceedance rate of wind speed at the time of maximum water level. Since water level and wind are correlated, the two exceedance rates are different. In Geerse *et al* (2006) the difference between these two exceedance rates was analysed. It was concluded that Hydra-K errs on the safe side for wind directions 210º-270º. The wind speeds at the maximum water level are about 10-15% lower than the wind speeds in the RW model. For directions 300º-360º, however, the wind speed at the maximum water level corresponds reasonably with the prediction from the RW model. Still, there are some differences of around 2 m/s for wind speeds between 15 and 20 m/s.

Combining the different contributions, we estimate that the uncertainty in the wind speed for return periods around 4000 years is about 20% (standard deviation). This is consistent with another study about wind modelling across the IJsselmeer (De Waal, 2003), in which it has been concluded that the overall uncertainty in the wind speed was 10-25%.

Wind direction

Hydra-K uses 12 wind-direction sectors of 30º each. This is based on the distribution of the RW model, which uses the same sectors for the wind speed exceedance rates. For reasons of convenience, the exceedance probability distributions of water level and wave period are also given separately for each wind sector. In this way, the probabilistic calculations in Hydra-K can be done for each individual wind sector separately thereby covering all possible winds.

A different number of wind sectors may lead to different results. Geerse *et al* (2006) investigated the effect of gradual aggregation of 10º-wind sectors to omnidirectional wind (one sector of 360º). Their conclusion was that the resolution of 30º sectors is adequate. Therefore, we do not consider any uncertainty associated with the choice of wind sectors.

Water level

The probabilities of extreme water levels are based on an extrapolation of the probability of exceedance distributions of the water levels at monitoring stations along the coastline (see Figure 6). Hydra-K uses conditional Weibull functions for 12 wind directions to describe the probability of exceedance of water levels at each water level station. The 12 wind directions combined give the total (or omnidirectional) probability of exceedance. The omnidirectional Weibull parameters for a number of stations in the Wadden Sea area are:

	HLD	TSW	ELD	HRL	LWO	DFZ
ω (-)	1.61	1.9	1.87	2.09	2.12	2.47
ρ (1/year)	3.254	3.32	5.781	5.175	6.139	4.182
α (-)	1.6	2.32	1.27	2.17	1.83	1.91
σ (m)	0.9012	1.5015	0.5357	1.5718	1.2515	1.635

The probabilities of exceedance of water levels for these stations are displayed in Figure 8. The locations inside the Wadden Sea (HRL, LWO and DFZ) clearly have higher water levels, due to the local wind set-up effect. This effect is strongest in DFZ, where the geometry of the Ems estuary causes a local wind setup for north-western winds.

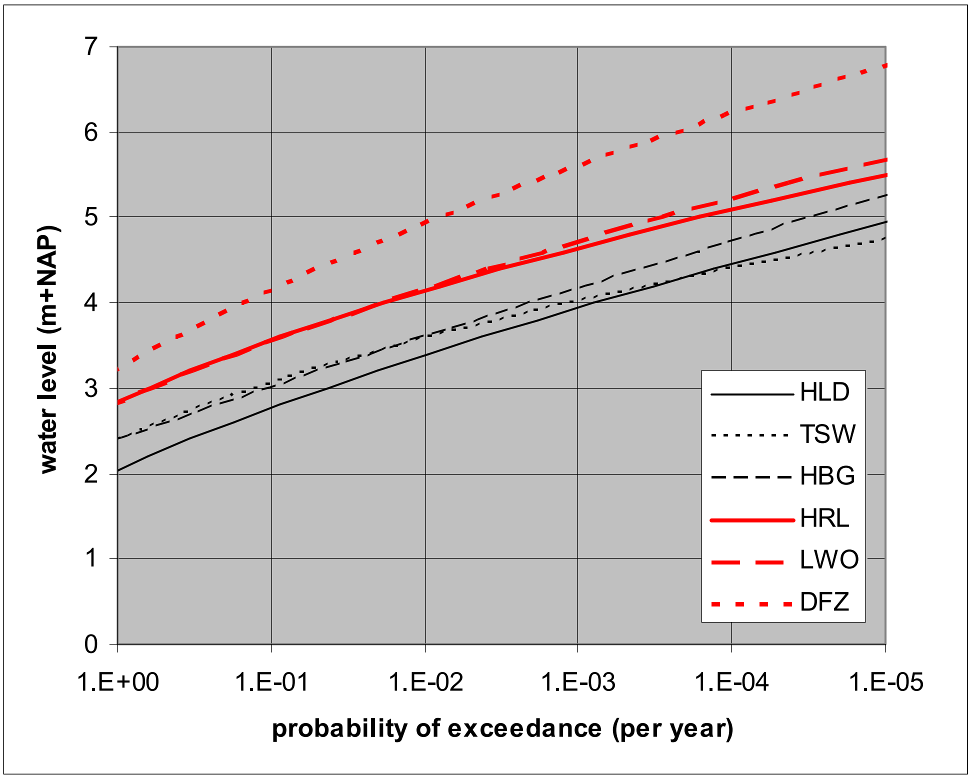

Figure 8: Probabilities of exceedance of water levels in the Wadden Sea area.

The extrapolation of water levels to extreme values and 4000 year return periods causes a number of uncertainties:

Firstly, the extrapolation requires a fitting function to the observed data of extreme surges. The conditional Weibull function is not the only option. Alternative fitting functions lead to different results in the 4000-year return levels. Dillingh *et al* (1993) have applied several fitting functions to the same data set of about 100 years of observations at several monitoring stations. The model uncertainty associated with the choice of the fitting function can be derived from the variance in the water level with a particular exceedance rate. The variance in the results from Dillingh for an exceedance rate of 10^4 years was about 4%, or 20 cm.

Secondly, the observational records of monitoring stations cover a relatively short period compared to the target return period of 4000 years. To estimate the probability of such extreme water levels requires an extrapolation far beyond the observed period. Due to the extrapolation of relatively few measurements to a return period of 4000 years, the statistical uncertainty in the extreme water levels is large (WL, 2005). Dillingh *et al* (1993) showed that this statistical uncertainty is about 40 cm for Delfzijl and 30 cm for Harlingen and Den Helder (standard deviations).

Van den Brink *et al* (2003) use a climate model to generate synthetic data for wind speeds. The storm surge at Delfzijl is related directly to the wind through a simple model (Timmerman, 1977). From generalized extreme-value (GEV) theory it follows that the statistical uncertainty in the surge at Delfzijl is of the order of 30% for 10.000 year return periods (standard deviation). We estimate this corresponds to about 20% or 1.3 m for 4000 year return periods. The uncertainty from the GEV analysis will be reduced by using more observations, instead of only the annual maxima. Also, the GEV is not the best fitting function to the data sets (Dillingh *et al*, 1993). For a conditional Weibull function, the fit will be better and the statistical uncertainty smaller. Based on these arguments we expect the total uncertainty for the 1/4000 water level at Delfzijl to be between 0.8 and 1 m (standard deviation).

Furthermore, the extrapolation from observed data does not contain information about possible future developments of a changing climate, induced by e.g. greenhouse gases. The mean sea-level rise is taken into account by making a correction to the water level probability distributions. The observed trend in sea-level rise continues to 2011. Based on the variation between the stations along the coast line and the standard error of the linear regression, we estimate the standard error in the mean sea level rising is about 1 cm (standard deviation) in all locations (see Figure 9). This is negligible compared to all other uncertainties in water levels.

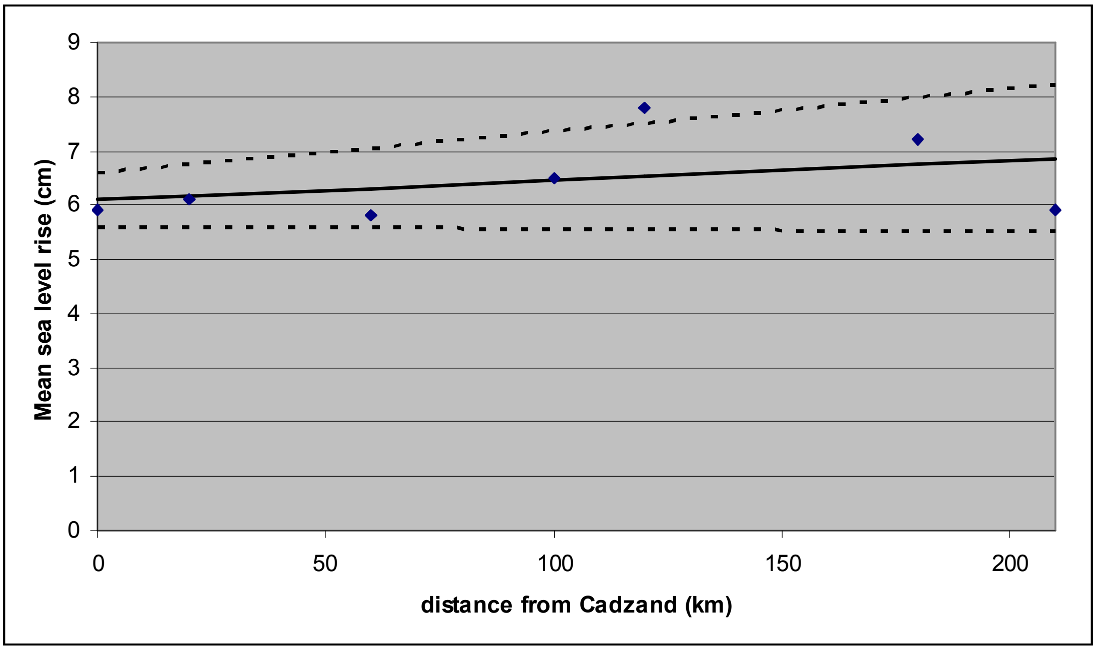

Figure 9: Correction for mean sea level rise along the Dutch coast line and uncertainty (1 std).

By using a probability of exceedance distribution based on historical data we assume that this distribution is time independent. There is no correction for a possible change in frequency of severe storms due to climate change. Bijl *et al* (1999) conclude there is no sign of a significant increase in storminess over North-Western Europe in the available observation data. Smits *et al* (2002) concluded that the storminess will decrease (!) with about 10% per decade, while NCEP-NCAR and ECMWF reanalysis data suggest an increase of storminess. Sigmond *et al* (2006) point out that west winds on the Northern hemisphere may become stronger during winter. However, this trend cannot be found in the observations: according to the IPCC2007 report there is a decline in stormyness from the late 1800's to 1960, then a maximum near 1990 and then again a decline up to 2006. Considering these inconsistent and mostly qualitative findings, it is very difficult to quantify the uncertainty related to this phenomenon. Therefore, we do not consider it in this study.

Finally, the extrapolation implicitly assumes that the high water levels are generated by a single stationary process, a common meteorological storm. A second population of rare but intense storms, from a different kind of meteorological origin, would result in higher return rates of extreme water levels than estimated from standard extreme-value analysis of the available observation records. This effect is pointed out by Van den Brink (2004). The phenomenon is still under investigation and at this moment we cannot quantify the uncertainty related to this effect. Therefore, we do not take it into account in the current study.

In WL (2007a), the uncertainty of the water level for a return period of 1000 years at Hoek van Holland was estimated as 70 cm (standard deviation). For location Den Helder the uncertainty was estimated smaller (50 cm), because the wind set-up at this location is typically smaller than at Hoek van Holland. For 4000 year return periods, the uncertainty at Den Helder will be larger again: we estimate about 60 cm. For other locations in the Wadden Sea, with larger storm surge set-up values, the uncertainty will be proportionally larger than the 60 cm value for Den Helder.

Weighing all the above arguments, we estimate the overall uncertainty (standard deviation) to be 60 cm for Den Helder, 70 cm for Harlingen/Lauwersoog, and 90 cm for Delfzijl. These values represent the uncertainty in the probability distributions of the water levels at return periods of around 4000 years.

2.2.6 Relationships between wind and waves (no. 6 in Figure 3)

In the Hydra-K version that will be used for the Wadden Sea, the offshore wave height, period and incident angle are directly related to wind speed and wind direction.

Wave height

Figure 10 shows the offshore significant wave height as a function of wind speed for two wind directions. The empirical relationships between wind speed and wave period ($T_{m-1,0}$) were derived from their marginal probability functions of exceedance (Stijnen 2005b). The wave height (H_{m0}) is then calculated as a power law function of the wave period:

$$H_{m0} = \left(\frac{T_{m-1,0}}{c} \right)^{1/d}$$

These relationships are assumed fully deterministic, i.e. there is no additional variation of wave height at a given wind speed. Figure 10 shows the functions for N and NW wind, as used by Hydra-K for the offshore location Europlatform. Similar relationships are determined for the other offshore stations.

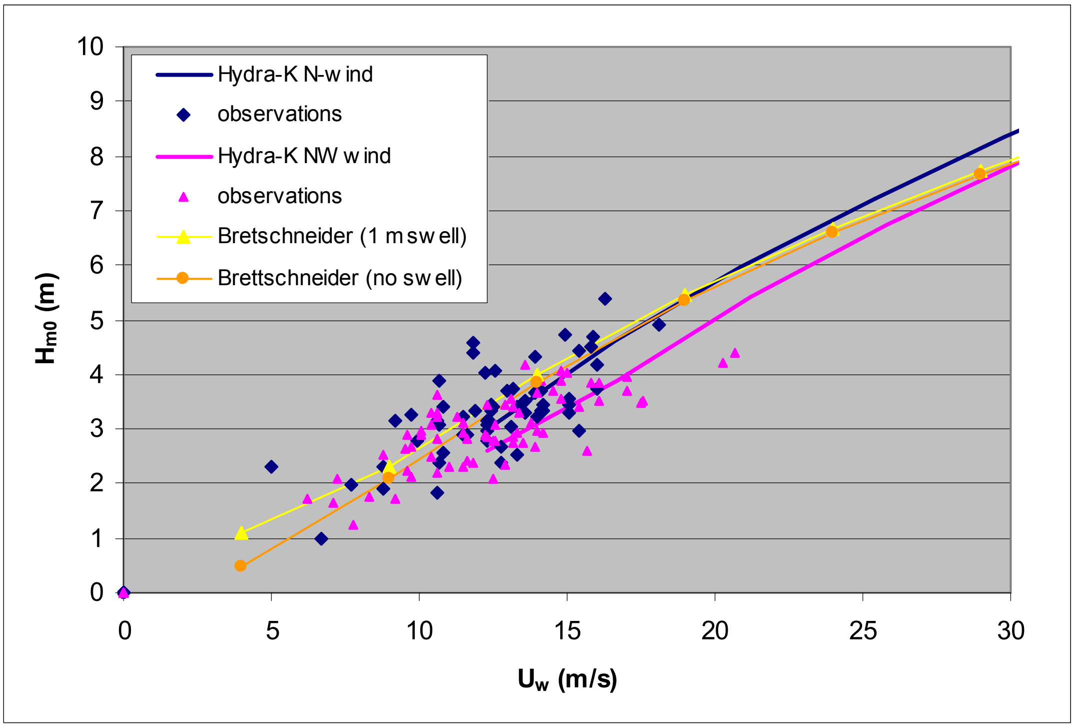

Figure 10: Wave height as a function of wind speed at the Europlatform station for wind directions N-NW. Bretschneider parameters are 50 m depth, 750 km fetch and 1 m swell.

The error in the wind-wave functions can be substantial, because variations in wind speed and storm duration are completely ignored. Figure 10 shows a number of observations and, for comparison, a Bretschneider relationship between wind speed and wave height (Bretschneider 1957, 1970). The spreading of the observations around the deterministic Hydra-K functions is calculated to be about 1 m (standard deviation). For extreme wind speeds the uncertainty will be larger, we estimate about 20%.

Waves over a bed level of -20 m+NAP (which is where the offshore waves are measured) are constrained by the water depth under extreme conditions. Therefore, the extreme wave heights are restricted, which is not accounted for in the HBC calculations (WL, 2007a). This restriction can lead to a systematic error, particularly at the SON station, which is relatively shallow. (See also Activity 0.2 of SBW Wadden Sea: Caires, 2006a,b).

The total uncertainty in the offshore wave height is estimated at about 20%. Part of this uncertainty is accounted for by the uncertainty in the wind speed (see 2.2.5). However, due to the weak dependency of the wave height on the wind speed (the slope in Figure 11 is about 0.25), this part is negligible. Therefore, we will apply an uncertainty in the wave height of 20% (standard deviation) in the SWAN uncertainty analysis (see Chapter 3).

For the Wadden Sea, the wave height at nearshore (shallow) waters is mainly determined by the nearshore bathymetry. Therefore, we expect that the effect of a possible error in offshore wave height on the nearshore wave height is limited.

Wave period

The spectral wave period ($T_{m-1,0}$) is also derived from the wind speed (Stijnen 2005b). Similar to the wave height, Hydra-K uses empirical relationships, depending on the wind direction (see Figure 11). The spreading of observations around the deterministic curves indicates that there is considerable uncertainty associated with this.

It is for this reason that in 2006 a version of Hydra-K was created in which $T_{m-1,0}$ was treated as an additional random variable. However, due to technical problems related to the extrapolation of results to extreme values (step 9), we decide for the moment not to use the wave period as a random variable.

The total uncertainty in the spectral wave period ($T_{m-1,0}$) was estimated at 20% in WL (2007a). One may argue that part of this spreading is accounted for by the uncertainty in wind speed (see 2.2.5). However, due to the weak dependency of the wave period on the wind speed (the slope in Figure 11 at high wind speed is only about 0.2), this part is negligible. Therefore, we will apply an uncertainty in the wave period of 20% (standard deviation) in the SWAN uncertainty analysis (see Chapter 3).

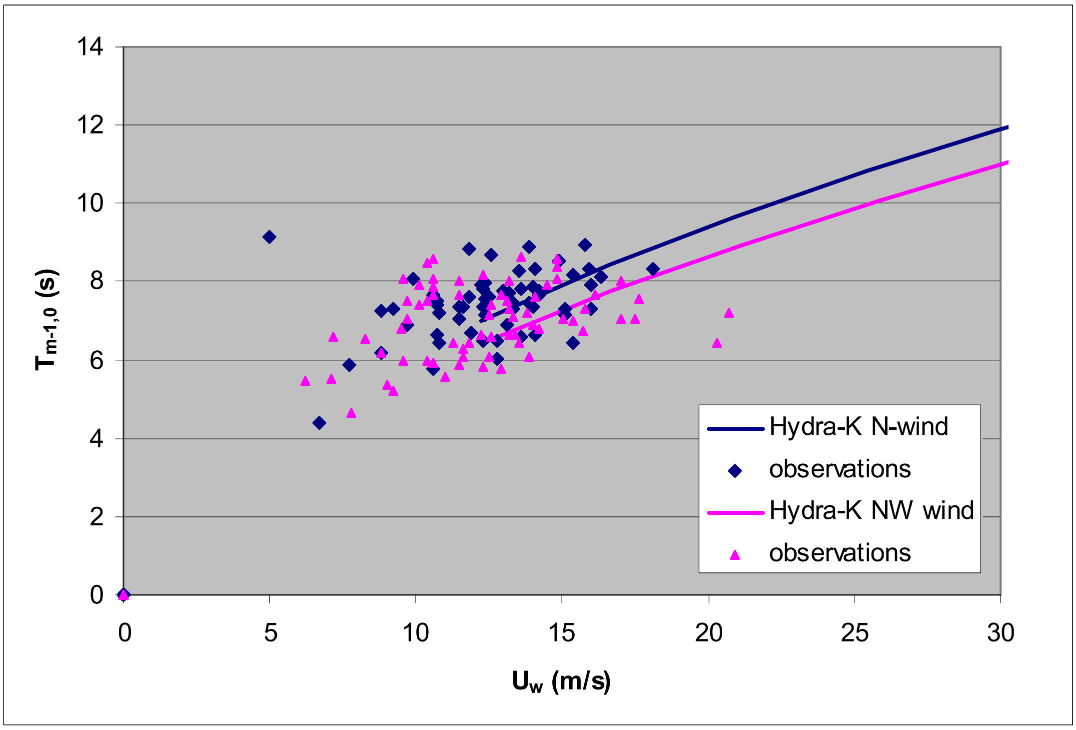

Figure 11: Spectral wave period as a function of wind speed at Europlatform.

Offshore wave-incident angle

The direction of the offshore waves is assumed equal to the wind direction at the time of maximum water level. This assumption introduces some uncertainty. The offshore wave field is the result of the wind over the past few hours and the wind may have changed direction. On the other hand, as the waves approach the shallow shoreline they will change direction as well. The angle of the nearshore waves is mainly determined by the nearshore bathymetry. Therefore, the uncertainty in the offshore wave angle is expected to be a minor source of error in the overall uncertainty.

Based on observations during a number of storms on the North Sea we estimate the error in offshore wave direction to be +/- 15º. This uncertainty will be accounted for in the SWAN uncertainty analysis (see Chapter 3).

2.2.7 SWAN parameter and model uncertainty (no. 7 and 8 in Figure 3)

The wave conditions at the sea defences result from computations with the wave model SWAN. This model translates offshore wave conditions, water levels and wind field to nearshore wave conditions.

A SWAN model of the Wadden Sea (Friesche Zeegat area) has been calibrated and validated against observations. The model is then formally applicable to normal conditions, comparable to the conditions during the observations. In Hydra-K, however, the model is employed to predict nearshore wave conditions for very extreme storms, generated by the 'De Haan' up-scaling. These conditions fall beyond the range of the calibration and validation data set.

In Chapter 3, the uncertainty in SWAN *parameter settings* will be addressed in further detail. While estimating the range of each parameter it will be kept in mind that the parameter uncertainty should correspond to severe storm conditions.

The *model uncertainty*, related to the validity of the basic model formulations and physical processes under extreme conditions, is difficult to quantify. Due to the lack of observations, we cannot assess to what extent the model formulations and parameter settings are still valid for a severe storm situation. For the current analysis, we do not consider this model uncertainty and we hope that a large part of the total uncertainty will be captured by the variation of parameter settings, as described in Chapter 3.

2.2.8 Nearshore waves from interpolation and extrapolation (no. 9 in Figure 3)

The results of a set of SWAN simulations are gathered in a database, the so-called 'KustDB2006'. This database is used by Hydra-K to translate the offshore wave characteristics to nearshore locations. The database usually contains SWAN results for water levels 2, 4 and 6 m+NAP and wind speeds 20, 25, 30, 35, 40 m/s.

For a particular up-scaled storm the nearshore wave parameters are calculated from the water level and wind by interpolation between similar results in the database. Suppose the wind speed of an up-scaled storm is equal to 37 m/s and the water level is 5.2 m. For this wind speed and water level no SWAN results are available. Therefore, Hydra-K interpolates between available results for wind speed 35 m/s and 40 m/s and water level 4 and 6 m, for the given wind direction. We need to perform a two dimensional (linear) interpolation (for U_w and h) between four computation results to obtain a value for H_{m0} and $T_{m-1,0}$.

In some cases the storm conditions are outside the range of SWAN calculations and the interpolation becomes an extrapolation. In case of a water level above the maximum value in the database (6 m) an extrapolation for U_w=35 m/s and 40 m/s is made separately. Next, interpolation is done between these to U_w-values (see Figure 12).

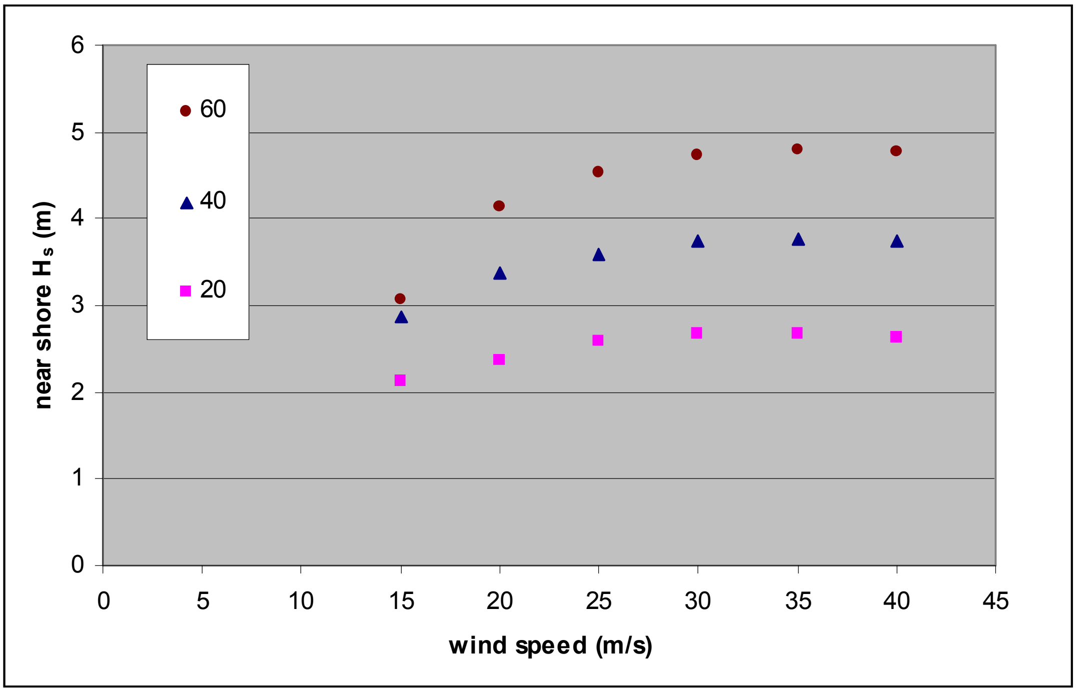

Figure 12: Part of the contents of the KustDB for the Dutch west coast. Wave height as a function of wind speed, for three values of water level (in dm). Wind direction is 330º.

The error that is made by linear interpolation can be estimated by comparing it to the result from a second-order interpolation, using the second derivative at 30 and 35 m/s. The difference between the linear and second order interpolations is given in Figure 13.

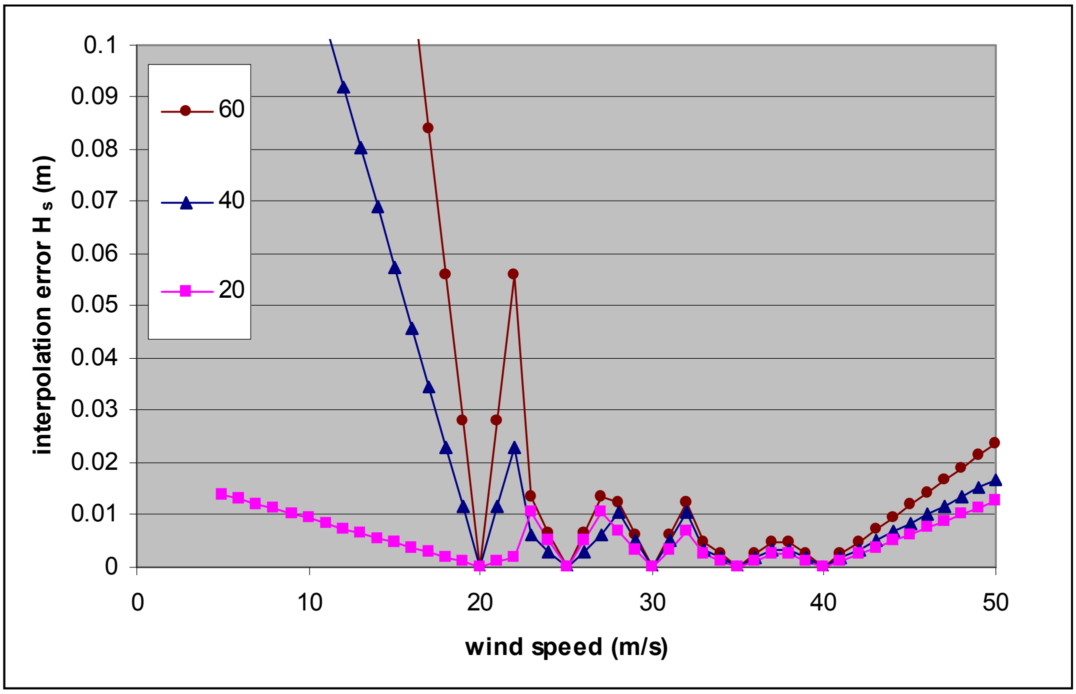

Figure 13: Difference between linear and second order interpolation as a measure for the interpolation error .

The errors are small within the range of the database (20-40 m/s). At most, the error is 6 cm, which is negligible compared to other errors. Outside these limits the interpolation becomes an extrapolation, and the error increases sharply. For wind speeds below 20 m/s the error increases a lot as a result of the large curvature of the H_{m0}-U_w function (see Figure 12).

The same analysis has been done for the spectral wave period, (see Figure 14). The interpolation error within the range of the database is limited to 0.1 s or less. Only outside the range of the database, the error may become non-negligible.

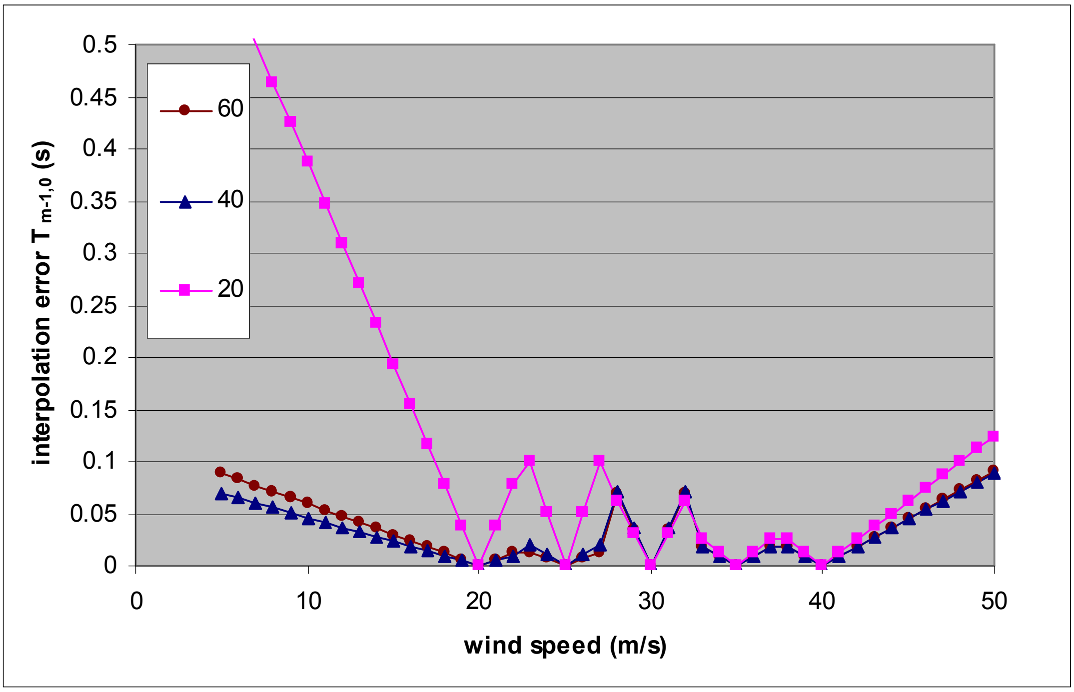

Figure 14: Difference between linear and second order interpolation error for the spectral wave period.

The above analysis shows that one should be aware of errors if the look-up values fall outside the range of the values in the database. In the HBC uncertainty analysis, however, we do not consider the interpolation error any further. The reason is that this uncertainty can easily be reduced by extending the range of the database by adding suitable additional SWAN computations.

2.2.9 Offshore to nearshore water level (no. 10 in Figure 3)

The water level at the sea defences is derived from up-scaled water levels at several monitoring stations along the coast. This has been done by linear interpolation between the three closest monitoring stations. For the Dutch western coast, with its almost straight shoreline and gradually varying water levels, this procedure is readily acceptable. No local effects are expected.

In the Wadden sea, the water level observations from stations at Den Helder, Harlingen, Lauwersoog and Delfzijl will most likely be used (see Figure 6). The coastline between these stations is more curved than the western coast and local effects may play a role due to the complex geometry and bathymetry of the area. Considering the geometry of the Wadden sea, we expect the strongest local effects at Delfzijl. For the Delfzijl area the water levels will be acceptable, because a monitoring station is located at Delfzijl. However, if we use the Delfzijl station for interpolation of water levels at other locations, for instance Eemshaven between Delfzijl and Lauwersoog, then the local effect at Delfzijl is wrongfully translated to that location.

An estimate of the magnitude of this effect can be made if we consider the storm surge of November 1st 2006. This storm caused an extremely high water level in Delfzijl, which was probably due to local wind effects. In Figure 15 we see that at Eemshaven, which is 15 km North-West of the monitoring station at Delfzijl, the observed water level is about 30 cm lower than the interpolated value between the observations at Delfzijl and Lauwersoog.

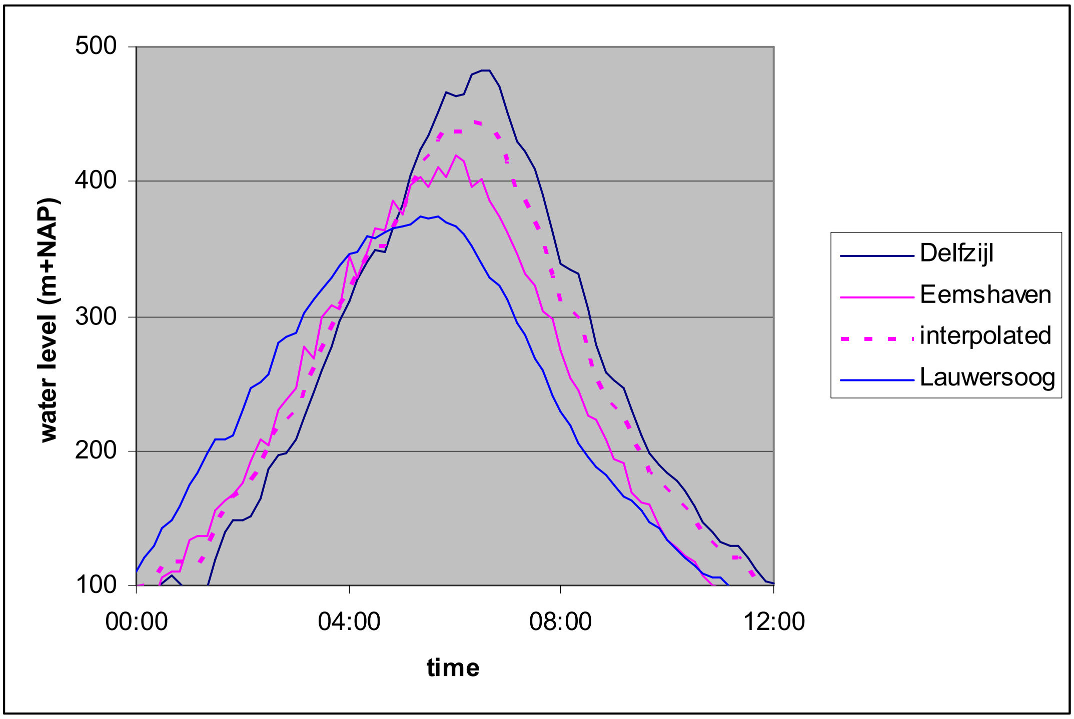

Figure 15: Water levels at DFZ, LWO and Eemshaven (observed and interpolated).

We estimate that this 30 cm deviation is about the *maximum possible error* for the Wadden sea. The example storm in Figure 15 showed an extremely strong local wind set-up, very specific to this location and wind direction. For different wind and for most other locations in the Wadden Sea the error will be smaller. The standard deviation of this error will certainly be much smaller than 30 cm. Considering the larger uncertainty in the water level caused by the extrapolation to extreme values (step 5), we do not consider this interpolation error in the overall uncertainty analysis.

On the other hand, we do recommend to further investigate this effect of possible interpolation errors in the water levels. If similar errors occur at other locations and situations, even if small, they can probably be corrected for with some simple modifications, such as a second order interpolation, or a location-specific correction for local wind setup.

2.2.10 Dike properties (no. 11 in Figure 3)

In order to calculate a failure rate, we need to know the relevant properties of the dike. For the failure mechanism 'wave overtopping', these properties are the cross-section, which consist of several line segments, the crest level and the roughness of each of the segments. Given these properties, we are able to calculate whether a dike fails at a certain water level and wave load. These calculations are done within Hydra-K, but they can also be done on a separate stand-alone version of the failure model, PC-Overslag (see Figure 16).

There can be considerable uncertainties in the properties of the dike. For example, the cross-section may vary along the dike. For the current study we assume that the properties are known exactly. The uncertainty in this part of the calculation is the subject of a separate study ('onzekerheidsanalyse faalmechanismen').

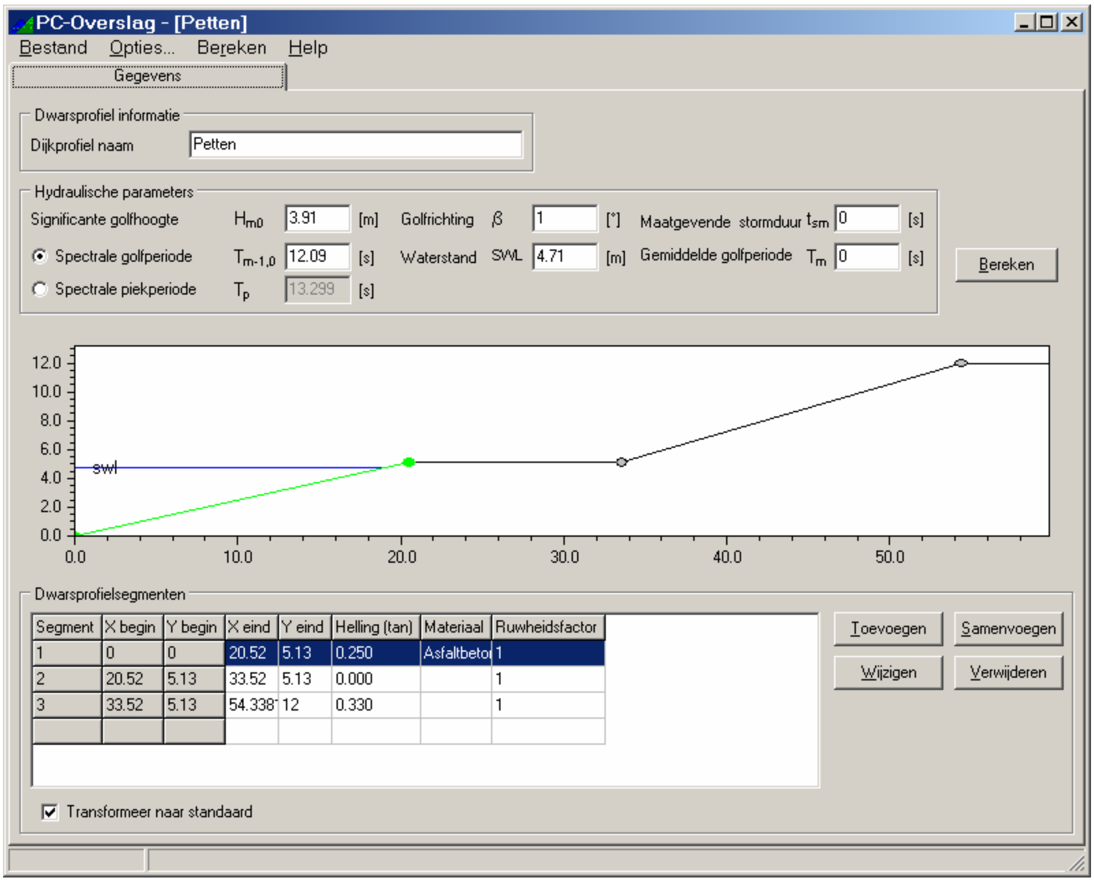

Figure 16: Stand-alone version of the failure model (PC-Overslag).

2.2.11 Failure-rate calculation (no. 12 in Figure 3)

Hydra-K has been developed for assessing coastal dikes on their crest level and revetment strength. Generally speaking, the description in Hydra-K of the failure mechanisms regarding the height of the flood defence (crest level) are fairly good. However, the description of failure mechanisms concerning the revetment strength is an important source of uncertainty (Ferdinand Diermanse, pers. comm.).

The selection of storm events of 24 years is relatively short to represent a return period of 4000 years. This causes a large statistical uncertainty, which can be estimated by assuming that the dike failure is a Poisson process of independent events. Although the final failure rate of our dike is predefined, in the sampling method it is based on 50 events. The variance in a Poisson sampling process is equal to the number of samples, so the standard deviation is $\sqrt{50} = 7.1$. The relative error in the failure rate is $\sqrt{50} / 50 = 14\%$.

The failure rate depends on the definition of failure. For the failure mechanism ‘wave overtopping’ in combination with sea defences the critical discharge is usually taken equal to 1 l/s/m. If more water spills over the crest, then the dike is said to fail.

An empirical model is used to calculate the amount of wave overtopping as a function of the water level and wave parameters. This empirical model is highly uncertain, but for this type of uncertainty a safety margin of a single standard deviation is usually applied. Moreover, if the dike formally fails, that is, the amount of water over the crest is more than the critical 1 l/s/m, in practice it will not fail completely right away. The ‘remaining’ strength is still thought to be considerable.

For this study we assume that the failure rate calculation is perfect. We only use the failure model to express the uncertainty in HBC as an uncertainty in a single quantity, i.e. the critical crest level.

We imagine a virtual dike with a straight asphalt slope of 25% (1 on 4). The failure mechanism is 1 l/s/m wave overtopping. The maximum failure rate is once per 4000 years, which is the default for the mainland coastline of the Wadden sea. The crest-height calculation is done deterministically and without considering any uncertainty. In practice, the failure rate or required crest level calculation is associated with a considerable uncertainty. The analysis of this uncertainty will be the subject of a separate activity, which is currently under preparation[3].

2.2.12 Critical crest level (no. 13 in Figure 3)

The uncertainty in the critical crest level is a measure for the total uncertainty of the HBC. The uncertainty in the crest level can be derived form the uncertainty in HBC, but not the other way around.

2.2.13 Illustration point (no. 14 in Figure 3)

The HBC are issued with an illustration point for each location. The illustration point represents all possible combinations of water level (h), wave height (H_{m0}) and period ($T_{m-1,0}$) that would cause failure of the sea defence and that collectively have a return period of 4000 years.

[3] ‘Onzekerheidsanalyse Faalmechanismen’, supplementary activity by GeoDelft within the SBW Waddenzee project.

The illustration point is only one combination of water level, and wave characteristics. But it is a very special one. On the one hand it is a combination which causes failure of the flood defence corresponding to a return period of 4000 years. However, there are infinitely many of such combinations. The illustration point is the combination that has the largest probability of occurring.

The uncertainty in the illustration point can differ from the uncertainty in the HBC and the critical crest level. For instance, the procedure to determine the illustration point could introduce some additional uncertainty. However, since the illustration point is only representative of the true HBC, we do not consider this any further.

Summary

Table 1 gives an overview of the steps in the HBC calculation and the associated uncertainties that will be taken into account in the uncertainty analysis.

Table 1: Uncertainty range in the input parameters

HBC Calculation step		Parameters	Uncertainty (standard deviation)	Action
1	Observations	Water level, h	< 5 cm	neglected
		Wind speed, U_w	10%	neglected
		Wave parameters	5º	neglected
2	Selection of storm events	-	?	investigated in another project
3	De Haan sampling method	-	?	investigated in another project
4	Standard failure rate	μ	?	beyond scope of the project
5	Marginal distributions	Wind speed, U_w	20%	yes
		Direction, α_w	< 30º	neglected
		Water level, h	70 cm	yes
6	Wind-waves relationships	wave height H_{m0}	20%	yes *)
		wave period $T_{m-1,0}$	20%	yes *)
		incident angle α	15º	yes *)
7-8	SWAN model and parameters	H_{m0}, $T_{m-1,0}$	see Chapter 3	yes *)
9	Interpolation in KustDB	H_{m0}, $T_{m-1,0}$	< 6 cm, < 0.1 s	neglected
10	Interpolation of water levels	h	< 30 cm	neglected
11-13	Failure rate calculation	μ	?	investigated in another project
14	Illustration point	h, H_{m0}, $T_{m-1,0}$, α	-	disregarded

*) The marked variables: offshore wave height, period and incident angle and the SWAN model parameters, will not be varied in the overall HBC uncertainty analysis. These uncertainties are accounted for in a separate SWAN uncertainty analysis (Chapter 3).

3 Uncertainty analysis of SWAN

3.1 Introduction

The wave model SWAN forms an important part of the HBC-chain and the uncertainties in the results of SWAN simulations contribute significantly to the overall uncertainty in the HBCs (WL, 2007a). Since SWAN is a complex model itself we discuss the quantitative uncertainty analysis separately from the rest of the HBC-chain.

Although we treat SWAN separately from the HBC-chain as a whole, we do take into account the specific way in which the model is used within this chain. Within the HBC-chain SWAN is used to translate extreme offshore wave conditions, water levels and wind fields to nearshore wave conditions. This implies the following for the uncertainty analysis:

- Our aim is the uncertainty in the wave conditions at the toe of the sea defences along the main land behind a tidal inlet. More specifically, we focus on the wave height and the wave period at the sea defences resulting from the SWAN simulations.
- The boundary conditions of SWAN are considered the extreme hydraulic offshore conditions, extreme water levels and extreme wind fields. The uncertainty in these conditions will significantly differ from the uncertainty in measured conditions.

In order to define an approach for the actual quantitative uncertainty analysis of SWAN we first list and quantify the sources of uncertainty considered (Section 3.2). In Phase 2 the analysis is performed with a SWAN model for a part of the Wadden Sea.

3.2 Quantification of uncertainties

3.2.1 Model inputs

The model inputs consist of the extreme offshore wave characteristics, the wind, the water levels, the currents and the bed topography of the Wadden Sea. These are discussed below.

Extreme offshore wave characteristics

The extreme offshore wave characteristics (height and period) are derived from statistical extrapolation of measurements. Referring to WL (2007a), the uncertainty in the observation of offshore wave parameters is estimated as 5% (standard deviation). However, the extrapolation of these measurements largely determines the overall uncertainty in the extreme offshore wave characteristics, as discussed in Chapter 2. The uncertainties involved in estimates of probabilities of extreme events are known to be relatively large (see e.g. Van den Boogaard *et al*, 2005). We assume that a standard deviation of 20% is a fair estimate, both for wave height (H_{m0}) and spectral wave period ($T_{m0-1,0}$).

Note that, in Hydra-K, the wave height and period are derived from the wind speed, which is also an uncertain quantity. However, due to the weak dependencies of wave height and period on the wind speed (Figure 10 and Figure 11), we apply an additional randomization of H_{m0} and $T_{m0-1,0}$.

Wind

The uncertainty in the wind speed and direction has been discussed in Section 2.2.5. The standard deviation of the wind speed at return periods around 4000 years is estimated to be 20%. The uncertainty in wind speed is accounted for in the overall HBC computation by a randomized U_w. This wind speed is used as input in the SWAN calculation and we do not apply a second randomization in the SWAN uncertainty analysis.

Water level

The uncertainty in the extreme water levels was discussed in Section 2.2.5. We estimate the overall uncertainty (standard deviation) to be 60 cm for Den Helder, 70 cm for Harlingen and Lauwersoog, and 90 cm for Delfzijl. These values represent the uncertainty in the probability distributions of the water levels at return periods around 4000 years. The uncertainty in water level is accounted for in the overall HBC computation. Therefore, we do not consider it as a random variable in the SWAN uncertainty analysis.

The water level in the Wadden Sea is assumed a flat surface in many SWAN calculations. In reality, however, the tidal dynamics and wind set-up cause the water level to be tilted. This can be clearly seen in Figure 16, where the tilt angle is shown as a function of water level at the coast. The tidal cycle can be identified as a circular pattern. At the moment of maximum water level, the tilt is usually positive (higher water level at the coast) and the tilt angle varies between 0.00001º and 0.00005º. For the uncertainty analysis we will consider the tilt angle a random variable with a uniform distribution between these values.

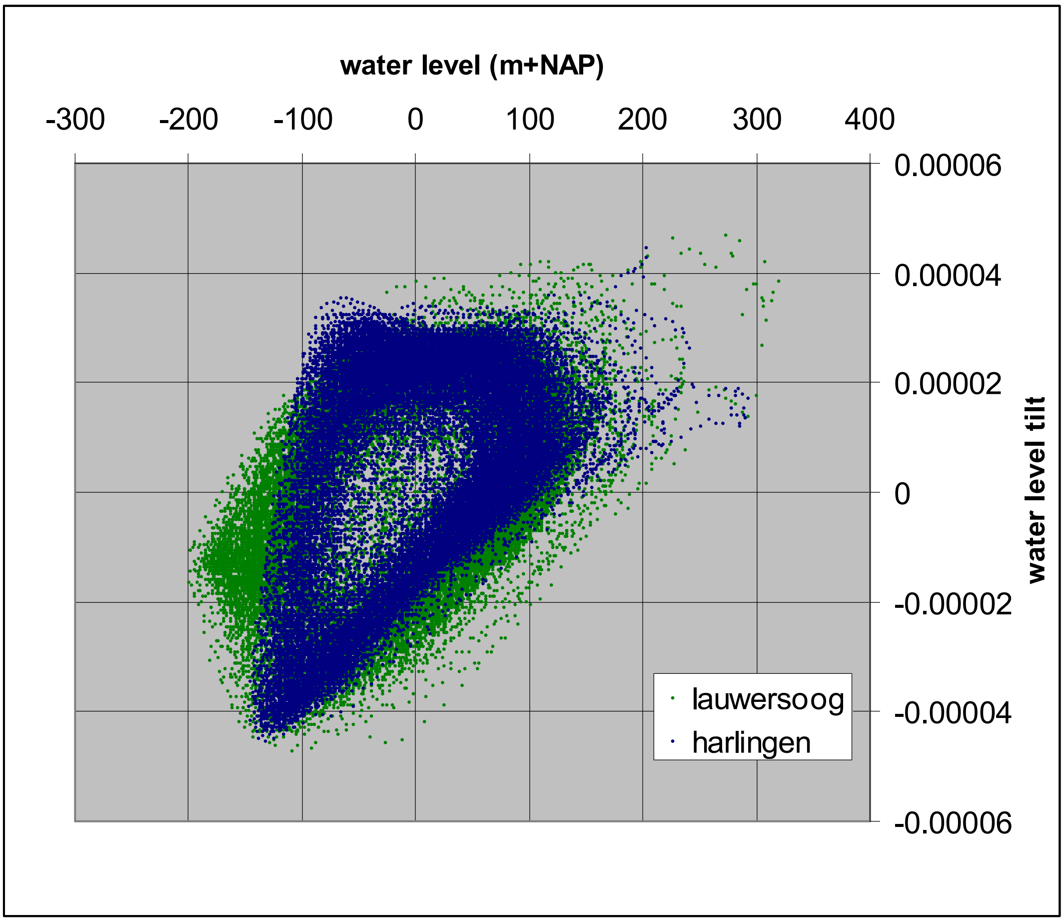

Figure 17 Tilt of the water level (angle) as a function of water level for two locations in the Wadden Sea. The calculated tilt is based on observations at monitoring stations.

Currents

Within the present project it is not feasible to vary the complete current field, since that would require a separate current field for every run and hence a separate run of the computationally demanding flow model WAQUA. The preparation of such a large number of current fields would require too great a computational effort, which is not feasible within the present project. Moreover, at this point, it is unclear how the current could be taken into account as a stochastic variable. However, the most important variations probably occur in the magnitude of the current, not the direction. Therefore it is decided to keep the vectors of the current field constant (in the sense of the direction of the current), and to vary only the magnitude of the current.

This approach is based on the assumption that the flow pattern is approximately the same, regardless of the storm condition. However, there are indications that the flow pattern in the Wadden Sea under extreme conditions can deviate significantly from the pattern under ‘regular’ storm conditions (Alkyon, 2001). At present, Alkyon is involved in a research project to investigate this assumption.

It is difficult to quantify the uncertainty in the magnitude of the current field, but assuming that there can be some error in the choice of the time instant of the current field a variation of plus or minus 30% seems reasonable. This value of 30% is based on the assumption that the tidal profile has a sinusoidal shape and that the error in the chosen time instant is at most 1:30 hr, which corresponds to a phase difference of 1/4 π of the tidal cyclus. The assumption of a sinusoidal shape seems justified, given the times series of the water level in the nearby stations Terschelling and Nes (WL, 2006a).

Bed topography

There are different sources of uncertainty in the bathymetry. The system flats and channels may have moved between two soundings (measurements). This corresponds to an uncertainty in the horizontal plane. There are uncertainties in the vertical plane as well. Compared to the former uncertainties, the uncertainty in the measurement of the bottom levels themselves are negligibly small. The main source of uncertainty is in the seasonal and other time-dependent variation in the bottom. For example, the temporal depth variations during a storm are unknown. To address this uncertainty, the following approach is proposed:

- Quantify the movement of the system of flats and channels in both X and Y direction (where X corresponds to the longitude direction and Y to the latitude direction) between loadings in two different years.
- Estimate the range of movement over a time span of six years. In the Waddenzee area the loadings are performed every six years. This means that a bottom is at most 6 years ‘outdated’.
- Consider the origin (x_0,y_0) of the SWAN bathymetry as a random variable which can vary between the range found above. The complete bottom is then translated horizontally over a certain distance.

Figure 18 shows a difference plot of the local bathymetry of 2003 and the bathymetry of 1997.[4] The black lines denote typical translations of (patterns of) gullies. If the difference plot shows a strong difference and, parallel to this ‘gully’ but some distance away, another gully with an opposite sign, this refers to a local translation of the gully. The figure clearly show how the flats and channels move sideward. The largest translations between 1997 and 2003 are approximately 400 m. Assuming that the translation can be in any direction, the uncertainty in the origin (x_0, y_0) is estimated at 200 m. In other words, the range for the origin of the computational domain (x_0, y_0) = [x_original -200, x_original +200; y_original -200, y_original +200]. The consequences of this will be part of the outcome of the uncertainty analysis.

4 The bathymetry of , e.g., 2003 means that the bathymetry is based on bottom measurements (“loadings”) that are carried out not later than December 31, 2003. Missing data is filled up with a hindsight of the 6 years. So in fact the bathymetry of 2003 is based on the measurements carried out between January 1, 1998 and December 31, 2003. If duplicate data is available, the most recent information is used.

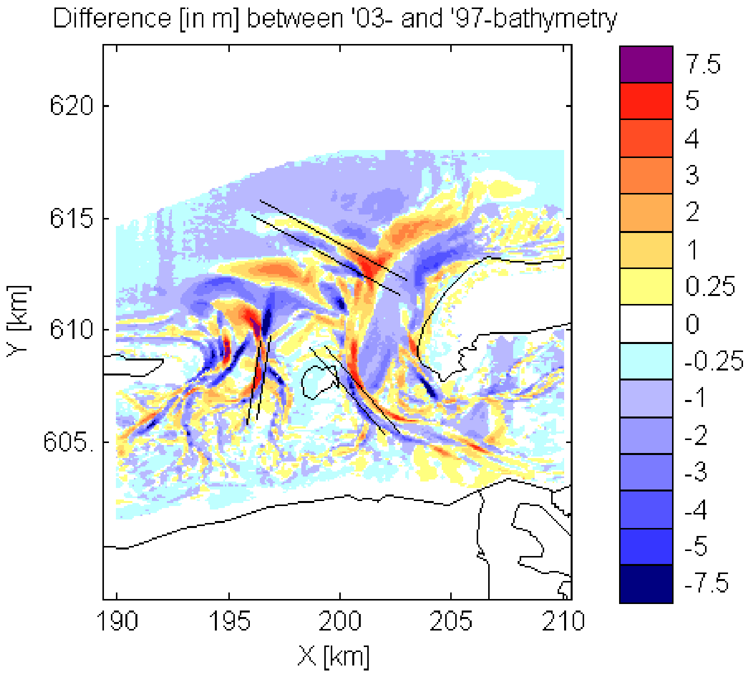

Figure 18 Difference between '2003 bathymetry' and the '1997' bathymetry near the Friesche Zeegat. Black lines denote typical translations of gullies.

Summary

Table 2 gives the uncertainty range in the input parameters.

Table 2: Uncertainty range in the input parameters

Process	Parameter	Uncertainty (range or standard deviation)
Wave boundary condition	H_{m0}	20%
	T_p	20%
	direction	15°
Bottom	x-origin	-200 - +200 m
	y-origin	-200 - +200 m
Water level	tidal range + set-up	70 cm *)
	tilt	0.00001 – 0.00005°
Current	direction	-
	magnitude	-30% to +30%
Wind	direction	15°
	magnitude	20% *)

*) The marked variables water level and wind speed are taken into account in the overall HBC calculation. For consistency, we use the randomized variables h and U_w as deterministic input in the SWAN uncertainty analysis. We do not randomize them a second time in the SWAN uncertainty analysis.

3.2.2 Model parameters

Table 3 presents the uncertain parameters that are identified in WL (2006b). Alternate formulations are available but these have not been taken into account in the present study. We choose to use only those formulations that are usually applied in the HBC-computations, because otherwise the amount of random variables would be too large. In order to be consistent with the other Ameland hindcast the default whitecapping expression of Komen *et al* (1984) has been replaced by the saturation based whitecapping formulation by Alves and Banner (2003), and recently adapted and implemented in SWAN 40.51 by Van der Westhuysen (WL, 2007b). This new formulation also uses a proportionality constant $C_{ds,wc}$. In addition a breaker parameter B_r is used, which indicates a threshold below which breaking ceases. For the latter parameter, the range of $1.5 – 2.0*10^{-3}$ is given in WL (2007b).

Table 3: Process categorization and the associated 10 uncertain parameters

Type	Process	Nr	Parameter	Explanation	Literature
Propagation in geographical space		--	*none*	based on linear wave theory	
Diffraction, depth- and current-induced refraction (propagation in directional space θ)		--	*none*	parameterised	Holthuijsen *et al*, (2003)
Shifting of radian frequency σ due to variations in mean current and depth (propagation in frequency space)		--	*none*	based on geometric optics approximation	
Deep water balance	Transfer of energy from wind to waves	**1**	α_{in},	wave growth parameter	Komen *et al*, (1984)
	Dissipation of wave energy due to white capping	**2**	$C_{ds,wc}$	proportionality constant	Komen *et al*, (1984)
		3	B_r	breaker threshold	Van der Westhuysen *et al* (2007)
	Nonlin. transfer of wave energy due to quadruplet (four-wave) interaction	**4**	C_{nl4}	proportionality constant	Hasselmann *et al* (1985)
		5	λ_{nl4}	frequency range of interaction	
Shallow water balance	Dissipation due to bottom friction	**6**	$C_{ds,bot}$	proportionality coefficient	Hasselmann *et al* (1973)
	Dissipation due to depth-induced breaking	**7**	α_{BJ}	measure for the breaking intensity	Battjes and Janssen (1978)
		8	γ_{BJ}	denotes where breaking starts	
	Nonlinear triad (three-wave) interaction	**9**	α_{EB}	proportionality constant	Eldeberky (1996), Janssen (2006)
		10	$f_{max,EB}$	high-frequency cut-off in triad computation	Van der Westhuysen (in prep.)

In the remainder of this chapter, the uncertainty in the different source terms is discussed and a range for the parameters is given. Note that this still requires a decision on how to translate the particular range to an uncertainty distribution. One could, for instance, consider the range as a 95% confidence interval. Assuming that the parameter is normally distributed, the accompanying standard deviation and mean can then be determined. If we choose to use the beta-distribution, the given range is not sufficient to determine the full distribution. It still requires an estimate for the mean and the standard deviation (or the skewness). The mean value is not problematic: this value can be assumed equal to the default setting. The determination of the value of the standard deviation requires some more research.

Deep water balance

The deep water processes include the source terms of wind input, white-capping dissipation and non-linear four-wave interactions (quadruplet interaction) which, together with the propagation terms, form the primary spectral evolution balance in (1) in deep water. The processes of wind input and whitecapping are modelled using the expressions of Komen *et al* (1984) and for quadruplet interaction the Discrete Interaction Approximation (DIA) of Hasselmann *et al* (1985) is applied. Both the expressions for wind input and whitecapping dissipation are linear in the variance density. Quadruplet interaction, on the other hand, is a nonlinear function of the variance density, and tends to impress a frontal shape (in frequency space) onto the spectrum. Quadruplet wave interactions therefore have a dominant role in imposing a self-similarity onto the wave spectra during all stages of development.

Of these three, the wind input expression, based on Snyder *et al* (1981), is the best-established experimentally - at least for light winds over a fairly mature wind-sea. Quadruplet interaction, although difficult to measure experimentally, is well-established theoretically for homogeneous, random-phase wave fields and a horizontal bottom. In operational applications, the DIA expression is used, which is an approximation of the complete set of quadruplet interactions described by Hasselmann (1962). The use of the DIA therefore introduces inaccuracies that are not insignificant, but the method is considerably faster than the full quadruplet calculation. In comparison to wind input and quadruplets, there is much uncertainty concerning the physical mechanism of whitecapping dissipation and hence the appropriate form for its source term. Therefore, the traditional expressions available for whitecapping were customarily used as a closing term in the calibration process. The new saturation based whitecapping formulation by Alves and Banner (2003), recently adapted and implemented in SWAN 40.51 by Van der Westhuysen (WL, 2007b) seems to be a promising improvement in this regard.

Considering the above, it is difficult, if not impossible, to give a straightforward uncertainty range of the parameters in the deep water source terms. These terms are calibrated using growth curves, such as derived by, e.g., Kahma & Calkoen (1992, 1994). The Kahma & Calkoen growth curves read:

$$\varepsilon_* = 6.5 \cdot 10^{-4} \cdot X_*^{0.9}$$

$$\nu_* = 3.08 \cdot X_*^{-0.27}$$

with $X_* = gX / u_*^2$, $\varepsilon_* = g^2 m_0 / u_*^4$, $\nu_* = \varpi_p u_* / g$, $u_* = \sqrt{C_D} \cdot U_{10}$.

In Young (1999) a different representation of the growth curves is given, including an indication of the confidence intervals of the growth curves:

$$\varepsilon = (7.5 \pm 2.0)\cdot 10^{-7}\cdot \tilde{X}^{0.8}$$
$$\nu = (2.0 \pm 0.3)\cdot \tilde{X}^{-0.25}$$
with $\tilde{X} = gX/u_{10}^{2}$, $\varepsilon = g^{2}m_{0}/U_{10}^{4}$ and $\nu = f_{p}U_{10}/g$

To get an estimation of the uncertainty in the deep water source term parameters, these confidence intervals are taken as point of departure. However, the growth curves as proposed by Kahma & Calkoen do not remain within these confidence intervals, which suggests that the given confidence intervals are too strict (see Figure 19 for a graphical presentation of the different curves).

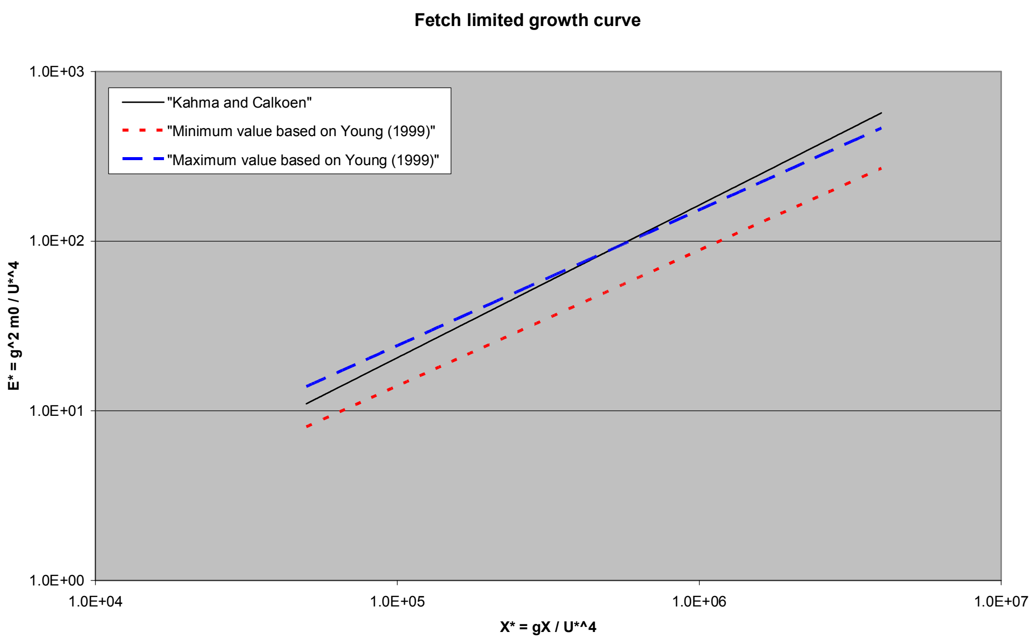

Figure 19 Fetch limited growth curves derived by Kahma & Calkoen and original confidence intervals based on Young (1999). X_* and E_* are the dimensionless fetch and wave energy.

Therefore, it has been chosen to apply the confidence intervals as derived by Young and to translate them to confidence intervals for the Kahma & Calkoen expression, resulting in the following expression:

$$\varepsilon_* = \left(6.5 \pm \tfrac{6.5}{7.5}\cdot 2.0\right)\cdot 10^{-4}\cdot X_*^{\,0.9} = \left(6.5 \pm 1.73\right)\cdot 10^{-4}\cdot X_*^{\,0.9}$$
$$\nu_* = \left(3.08 \pm \tfrac{3.08}{2.0}\cdot 0.3\right)\cdot X_*^{\,-0.27} = \left(3.08 \pm 0.46\right)\cdot X_*^{\,-0.27}$$

Figure 20 shows the Kahma & Calkoen expression with the adapted confidence intervals. Although this approach is, strictly speaking, not fully sound, for the present purpose it seems justified since the confidence intervals are merely used to get a rough estimation of the variation in the deep water source term parameters and not to accurately assess the uncertainty in the growth curves.

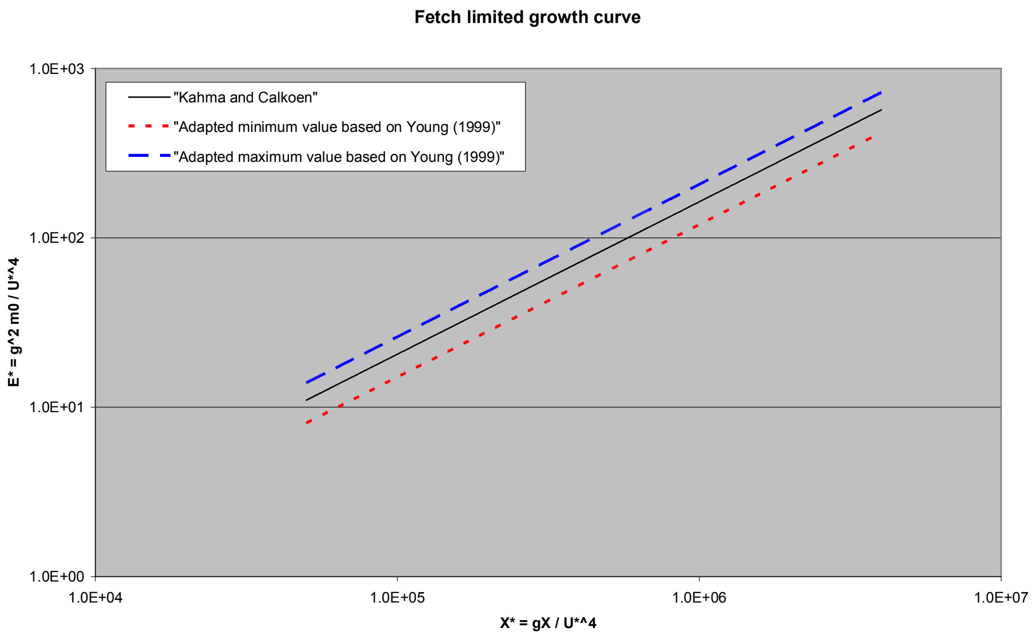

Figure 20 Fetch limited growth curves derived by Kahma & Calkoen and adapted confidence intervals based on Young (1999)

The deep water source term parameters of SWAN are varied such that the SWAN results remain within the adapted confidence intervals. The values of the parameter that correspond to the limit situation (i.e. the situation in which the SWAN result just remains within the confidence intervals of the growth curves) are assumed to define the range within which the parameters can be varied. Since uncertainty in the expression for the wind input is negligibly low compared to the other deep water source terms, the uncertainty in the expression for the wind input have not been taken into account in the present uncertainty analysis.

Note that for shallow water not much information on the wind input is available. However, even in shallow water, the uncertainty in the wind input (i.e., the magnitude and the direction) is significantly higher than the uncertainty in the parameters in the wind input source terms. Therefore, also in shallow water, the omission of the wind input parameters in the list of uncertain parameters and input variables seems justified.

Summary

Table 4 gives the default value and the range of the parameters in the deep water source terms.

Table 4: Uncertainty range in deep water source terms

Process	Parameter	Uncertainty
Transfer of energy from wind to waves	α_{in}	small compared to other source terms (personal communication Van der Westhuysen)
Dissipation of wave energy due to whitecapping	$C_{ds,wc}$	default = 5.E-5 range: 4.2E-5 – 5.5E-5
	B_r	default = 1.75E-3 range: 1.5E-3 – 2.0E-3
Non-linear transfer of wave energy due to quadruplet (four-wave) interaction	C_{nl4}	default = 3.E7 range: 2.5E7 – 3.5E7
	$\lambda^{*)}$	0.20 – 0.30 (uniformly distributed)

*) The deep water source term ‘quadruplets’ has a proportionality constant to scale the total amount of energy related to the particular source term. In order to assess the uncertainty in this source term, the proportionality parameter is the most straightforward parameter to use. The uncertainty in the remaining parameter λ lacks a clear empirical underpinning. However, varying this would significantly affect the shape of the wave energy spectrum (and hence, the wave period) and it is therefore not a parameter that can be neglected. Alkyon (2003) carried out a calibration study and used values in a range of 0.20 – 0.30, based on findings of Hashimoto and Kawaguchi (2001). For the present study, the same range has been adopted.

Shallow water balance

The balance of source terms in water of finite depth is more complex and not as well studied as the balance in deep water mentioned above. The dissipation processes induced by bottom 3friction and depth-induced breaking are modelled using turbulence and hydraulic jump (bore) analogies respectively.

Little is known about the mechanism of these dissipation processes, and the expressions are therefore speculative. Nonetheless, the source term for depth-induced breaking of Battjes and Janssen (1978) has proven robust in a wide range of applications. This expression has two parameters, namely α_{BJ} and γ_{BJ}. For bottom friction dissipation, the expression of Hasselmann *et al* (1973) is used. This expression has a single parameter in the form of a proportionality coefficient $C_{ds,bot}$.

Compared to the deep water source terms, the shallow water source terms are less uniform in the sense that the uncertainty of the different source terms cannot be determined in one and the same way.

Bed friction
The bed friction models that have been selected for SWAN are the empirical model of JONSWAP (Hasselmann *et al*, 1973), the drag law model of Collins (1972) and the eddy-viscosity model of Madsen *et al* (1988). The formulations for these bed friction models can all be expressed in the following form:

$$S_{ds,b}(\sigma,\theta) = -C_{ds,b}\,\frac{\sigma^2}{g^2\sinh^2(kh)}\,E(\sigma,\theta)$$

in which $C_{ds,b}$ is a bed-friction coefficient that generally depends on the bed orbital motion represented by U_{rms}:

$$U_{rms}^2 = \int_0^{2\pi}\int_0^{\infty} \frac{\sigma^2}{\sinh^2(kh)}\,E(\sigma,\theta)\,d\sigma\,d\theta$$

In the present uncertainty analysis the empirical model of JONSWAP is used. Hasselmann *et al* (1973) found from the results of the JONSWAP experiment $C_{ds,b} = C_{JON} = 0.038 m^2s^{-3}$ for swell conditions. Bouws and Komen (1983) selected a bed friction coefficient of $C_{JON} = 0.067 m^2s^{-3}$ for fully developed wave conditions in shallow water. Both values are available in SWAN. Bouws and Komen state that it is not possible to quantify the error in the bed friction.

In Shemdin *et al* (1977) a comparison is made between the different bed interaction mechanisms that can effect the waves, such as percolation, linear wave-bed interaction, bed friction and bed scattering. According to the authors the friction coefficient $C_{ds,b}$ can vary throughout the range 0.007 – 0.5 m^2s^{-3}. They state that the local ripples are important in determining the friction coefficient and they suggest a variability over two orders of magnitude. Taking into account two orders of magnitude would result in a range of approximately 0.0038 – 0.38 m^2s^{-3} for swell conditions and 0.0067 – 0.67 m^2s^{-3} for wind sea conditions or 0.007 – 0.38 m^2s^{-3} and 0.007 – 0.5 m^2s^{-3} if we include the upper and lower limit of 0.007 and 0.5 m^2s^{-3}.

In the test cases described in Shemdin *et al* (1977) the variability of the bed friction coefficient is less than the general variability described above. For the Marineland test at the Florida Atlantic Coast the bed friction coefficient was calculated in the range of 0.006 – 0.010 m^2s^{-3} and for a test case at the Melbosstrand (Cape Town, South Africa) the bed friction coefficient was found to be in the range of 0.06 – 0.10 m^2s^{-3}.

So, if we assume a similar variability as in the test cases described by Shemdin *et al*, the bed friction coefficients are approximately in the range of 0.03 – 0.05 m^2s^{-3} for swell conditions and 0.05 – 0.1 m^2s^{-3} for wind sea conditions. Note that these values are based on measured storm conditions and not on extreme conditions. During extreme conditions the importance of bottom friction can be different than during measured storm conditions.

Depth induced breaking

Ruessink *et al* (2003) derived a locally varying relationship between the wave-to-depth ratio γ and the product of the local wave number *k* and the water depth *h*, based on empirical data measured at Duck (NC, USA), Egmond and Terschelling: $\gamma_{rues} = 0.76kh + 0.29$. The relation is valid for *kh*-values within the range 0.25 – 0.75, resulting in the following range for γ_{BJ}: 0.48 – 0.86. In the paper, a graphical presentation of the uncertainty of the relationship γ versus *kh* is given, yielding in a slightly wider range of observed values of γ_{BJ}: 0.44 – 0.92.

It is recommended to keep the value of α_{BJ} equal to the default value 1.

Non-linear triad interaction
At the moment, the uncertainty in the non-linear triad interaction is lacking a thorough physical background. Estimates of the uncertainty in the parameter α_{AE} can not be soundly underpinned with empirical data. Therefore it is chosen to account for the uncertainty in the triad interactions with an on/off switch, which means that half of the computations is done with the triads (with the default settings) switched on, and half of the computations with the triads switched off.

Summary

Table 5 gives the default value and the range of the parameters in the shallow water source terms.

Table 5: Uncertainty range in shallow water source terms

Process	Parameter	Uncertainty
Dissipation due to bottom friction	$C_{ds,bot}$	default: 0.038 m^2s^{-3} (swell) and 0.067 m^2s^{-3} (wind sea) range swell: ≈ 0.03 – 0.05 m^2s^{-3} range wind sea: ≈ 0.05 – 0.1 m^2s^{-3}
Dissipation due to depth induced breaking	α_{BJ}	-
	γ_{BJ}	default: γ_{BJ} = 0.73 range: 0.44 – 0.92
Non-linear triad (three-wave) interaction	α_{AE}	on/off switch
	$f_{max,\ EB}$	

3.3 Case selection: Friesche Zeegat

To investigate the uncertainty in the SWAN results in a situation with a complex bathymetry in combination with tidal currents, the test case of the Friesche Zeegat seems to be a suitable case in terms of computational costs. Compared to other (similar) test cases, such as the present hindcasts in the Amelander Zeegat and the Norderneyer Seegat, the number of grid points in this test case is relatively small. The Friesche Zeegat test consists of three cases, one with a strong flood current (F51-01), one with a high water (F51-02) and one with an ebb current (F51-03). The latter has been selected because an ebb current significantly affects the wave field, even more so than a flood current, making this a very 'demanding' test case from a modeller's point of view. Since the aim of the present study is to quantify uncertainties and not to make a comparison with field measurements, the use of the most recent local bathymetry is not required.

In the ONR test bed (WL, 2002) the area is modelled on a grid with a spatial resolution of 250 m in x-direction and 200 m in y-direction, resulting in a grid of 124 by 94 points. Since the test case is relatively old, a verification run has already been carried out with the, at the time of writing, most recent version of SWAN (version 40.51A). This verification run on a grid with a grid spacing of dx = 125 m and dy = 100 m (248 by 188 points) and the settings similar to those in the test bed resulted in deviations from the original computation of less than 2% in terms of wave height and less than 0.2 s in terms of wave period, indicating that the original model schematization is sufficiently accurate (as far as the numerical resolution is concerned). A second verification run has been done in which the resolution was again doubled (dx = 62.5 m and dy = 50 m). The differences between the first and the second verification run were of the same order of magnitude as the differences between the run with the original resolution and the first verification run, indicating (again) that the run based on the original model schematization is sufficiently accurate. Table 6 shows the results of the three runs at 5 buoy locations.

Table 6: Comparison results on three grids with varying resolution

Buoy #	Depth [m]	Original spatial resolution (dx = 250 m; dy = 200 m)				First refinement (dx = 125 m; dy = 100 m)				Second refinement (dx = 62.5 m; dy = 50 m)			
		H_{m0} [m]	T_{m01} [s]	T_{m02} [s]	T_{m-10} [s]	H_{m0} [m]	T_{m01} [s]	T_{m02} [s]	$T_{m-1,0}$ [s]	H_{m0} [m]	T_{m01} [s]	T_{m02} [s]	$T_{m-1,0}$ [s]
2	8.0	2.1	5.5	4.5	7.0	2.1	5.8	4.8	7.2	2.0	6.0	5.1	7.4
3	7.0	2.1	5.8	4.5	7.5	2.1	5.9	4.7	7.6	2.1	6.1	4.9	7.7
4	10.9	0.5	2.2	1.9	2.8	0.5	2.3	2.0	2.9	0.5	2.5	2.2	2.9
5	13.2	0.9	3.4	2.8	4.3	0.9	3.5	3.0	4.1	0.9	3.6	3.2	4.1
6	9.8	0.5	2.1	1.7	2.6	0.5	2.1	1.7	2.7	0.5	2.3	1.8	2.8

The computing time required for one run with a grid spacing of 250 m is approximately 5 minutes on a Pentium 4 computer with 1.024 MB RAM internal memory and a 3.6 GHz processor. A run with a grid spacing of 125 m takes around 15 minutes and for a grid spacing of 67.5 m the (wall clock) time was approximately 40 minutes.

For the Friesche Zeegat area, we propose the following range for the Hydra-K database:

Variable	Nr values	Values
Water level h	3	2, 4, 6 m+NAP
Wind speed U_w	6	15, 20, 25, 30, 35, 40 m/s
Wind direction	5	300-330, 330-360, 0-30, 30-60, 60-300º

For each combination of variables a SWAN calculation will be done. The results (nearshore wave height, period and wave incident angle) are stored in the database. For the range mentioned above the database will thus require 3*6*5=90 SWAN runs. The uncertainty analysis will require at least an additional 100 runs in the Monte Carlo analysis (see Chapter 4). The number of SWAN runs is then 190 SWAN runs. For the high resolution grid (67.5 m grid spacing) this would amount to more than 5 days of total computing time.

In order to save computing time we will use an efficient iteration scheme (WL, 2007b) and an optimal convergence criterion. Note that the default convergence criteria, as used in the ONR test bed, are not sufficiently strict for the Wadden Sea.

4 Approach for quantitative uncertainty analysis

4.1 General approach

The uncertainty analysis of the HBC will be done by using a Monte Carlo sampling technique. Monte Carlo methods are a standard approach to uncertainty analysis of systems with many variables, that cannot easily be solved analytically. A Monte Carlo algorithm uses (pseudo) random numbers to generate many realizations of the same calculation. Each of the uncertain model parameters is sampled randomly from prescribed probability distributions. For each of these samples a simulation is performed, resulting in an ensemble of outputs. By statistically evaluating these random outputs we obtain information of the uncertainty of the output.

In the case of the HBC calculation, we use three separate Monte Carlo sampling steps for three different parts of the calculation that are associated with the main sources of error (see below). This will enable us to distinguish between the uncertainty introduced by each part. The results can be used to estimate which reduction in the total uncertainty can be obtained by reducing one of the sources of uncertainty.

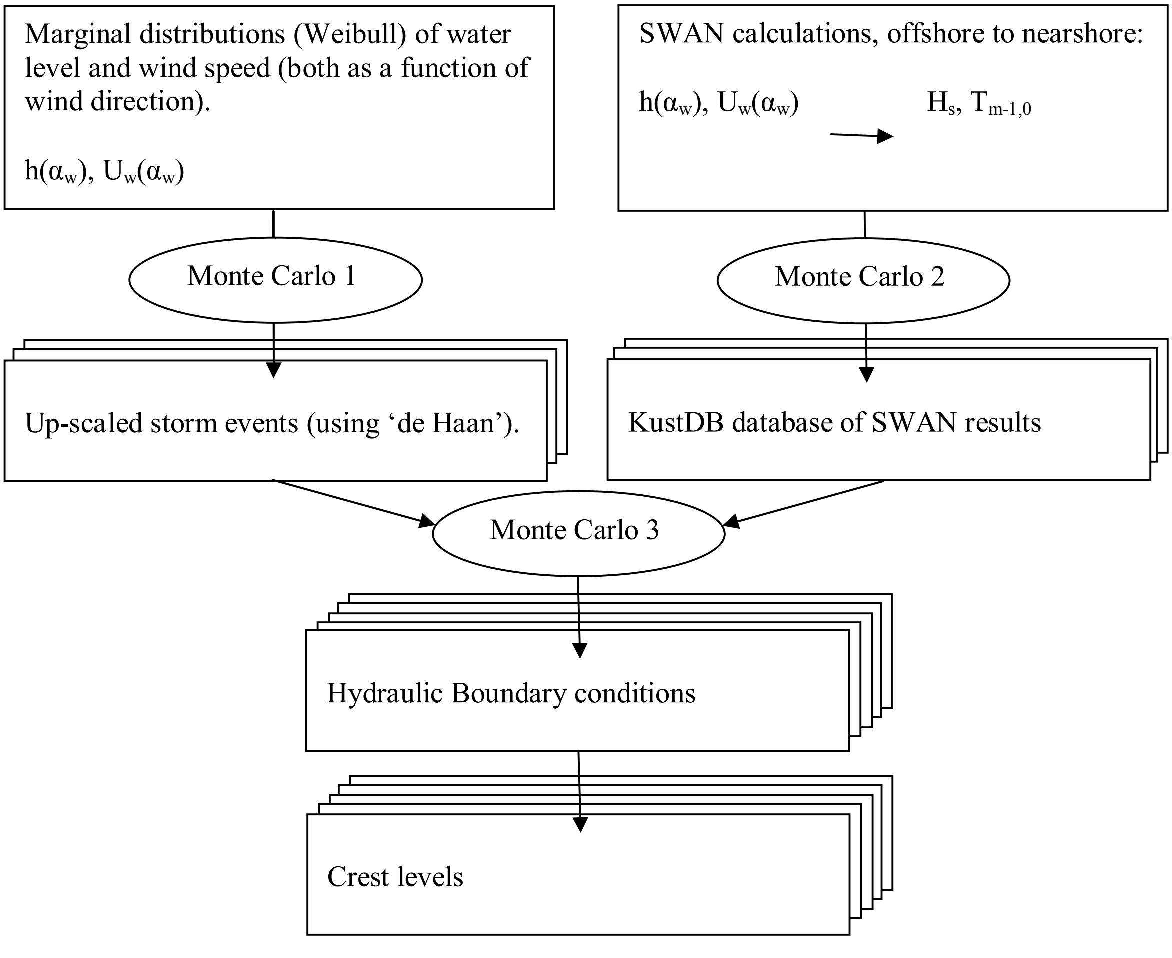

The uncertainty in the crest level is estimated by using the variance of the Monte Carlo sample results. The more samples we take the more accurate this estimate will be. The variance typically converges linearly with inverse of the number of samples[5]. The standard deviation, defined as the root of the variance, therefore converges with the inverse of the square root of the number of samples. For an estimate of the uncertainty (standard deviation) within 10% accuracy we expect to at least 100 samples. In the three Monte Carlo runs mentioned before we will initially use 100 samples. By observing the convergence behaviour as the number of samples increases, we will decide whether to take more samples.

4.2 Probability distributions

For most (if not all) of the uncertain parameters in the SWAN and HBC calculation no probability distribution are 'known'. For most uncertainties we estimate a mean and a range or minimum and maximum value (end points a and b), often based on (subjective) expert judgement. To translate this information into a probability distribution requires the choice of a distribution type and, depending on the probability distribution chosen, a variance σ^2 and a mean μ and/or other (scale or shape) parameters.

The uniform distribution is the most simple continuous probability distribution. It has constant probability density on the interval between the end points (a, b) and zero probability density elsewhere. Hence, in this model, every value - from the minimum to the maximum - is equally likely. For most real-world applications this distribution is not realistic. It is more likely that the probability density near the mean value μ is higher than the probability near the (observed) minimum and maximum values.

Due to implications of the central limit theorem, the normal distribution is arguably the most important probability distribution. It is completely characterised by a mean μ and variance σ^2. The central limit theorem states that the mean of any set of variables with any distribution having a finite mean and variance tends to a normal distribution. Many common attributes such as test scores, height, etc., follow roughly normal distributions, with few members at the high and low ends and many in the middle. Therefore, we choose the normal distribution for most of the uncertainty terms in the SWAN and HBC uncertainty analysis.

In some cases, however, the normal distribution poses a problem, since the distribution is not defined on a bounded domain. This implies that parameters may become negative, which is unrealistic for some parameters (the coefficients in the SWAN source terms for example). Moreover, the normal distribution is symmetric, which might not be realistic in certain cases.

Therefore, a third distribution is considered: the beta-distribution. The beta-distribution is defined in terms of two location parameters a and b (the end points mentioned before), and two (positive) shape parameters p and q. The latter (rather technical) parameters can be translated into the mean μ and variance σ^2 of the distribution. The beta-distribution has the following advantages:

5. Although there may be other reasons for slower convergence.

- the distribution is defined on a bounded domain, so, e.g., positive values can be guaranteed;
- the distribution is symmetric when $p = q$, while for $p \neq q$ skewness properties of the distribution can be included.

For the uncertainty analysis of SWAN and the HBC, we will use the normal distribution as the default distribution. For parameters with a bounded domain a beta distribution will be used.

4.3 Monte Carlo 1: Marginal distributions

The choices for the probability of exceedance functions for wind speed and water level have been identified as one of the main sources of uncertainty (see Section 2.2). The uncertainty in the up-scaled extreme wind speed has been estimated at 20% for return periods of 4000 years. The standard deviation in water level was estimated at 70 cm for Harlingen and Lauwersoog.

These uncertainties propagate into the wind speed and water level of the ‘de Haan’ up-scaled storms. This is visualized in Figure 21.

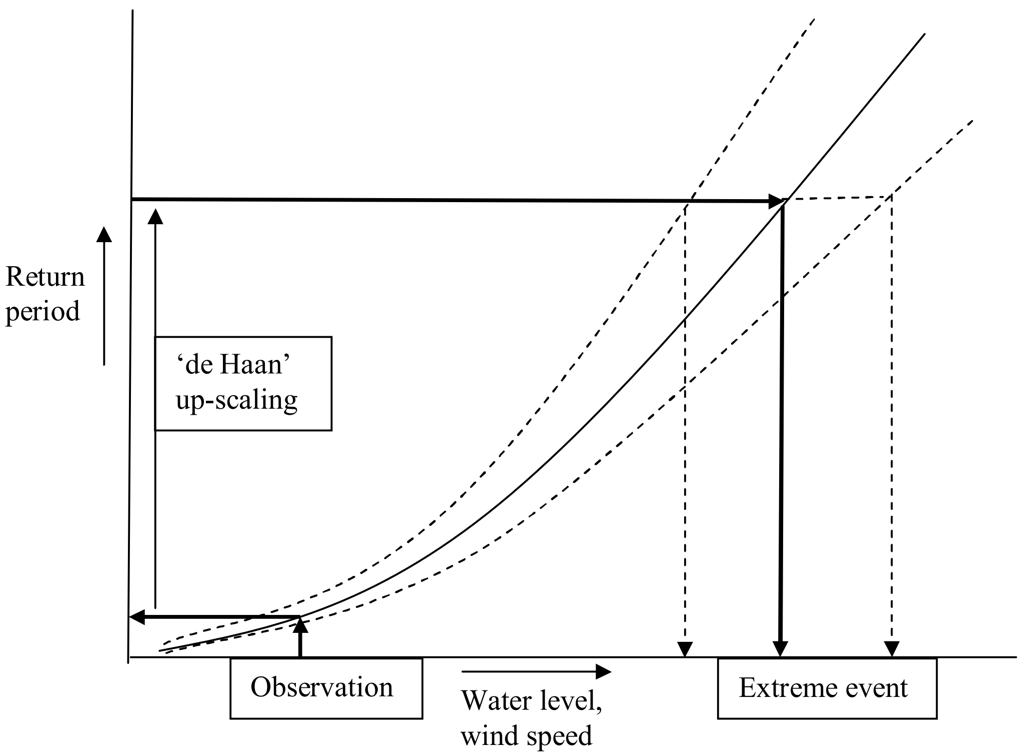

Figure 21 Uncertainty in water level and wind speed of an extreme event as a result of uncertainty in the exceedance rate probability function.

In fact, there is also some uncertainty in the estimate for the return period of the *observed* storm event. However, this uncertainty is much smaller than that for the extreme event, so we consider only the latter.

The uncertainty associated with the exceedance probability functions will be represented by adding a random 'shift' to all water levels and a 'noise factor' to the wind speeds of the up-scaled storms:

- The wind speed noise factor is $1+\varepsilon$, with ε drawn from a normal distribution with zero mean and a standard deviation of 0.2. The wind speeds of all the up-scaled storms are multiplied by this factor.
- The shift in the water level is drawn from a normal distribution with zero mean and a standard deviation depending on the location. For the Friesche Zeegat we use 70 cm. This shift is added to the water levels of all uscaled storms.

The 'random shift' and 'noise factor' are drawn independently. Although water level and wind speed are clearly correlated, their marginal distributions are derived independently. Therefore, the uncertainties in the distributions are also uncorrelated.

We propose to draw a total of 100 sets of up-scaled storms, each with shifted water levels (100 random numbers) and perturbed wind speeds (another set of 100 random numbers). The result is an 'ensemble' of extreme storm events, which will be used as input for the next step in the uncertainty analysis (Monte Carlo 3).

4.4 Monte Carlo 2: uncertainty analysis of SWAN

Uncertain parameters

In the uncertainty analysis of the SWAN model the uncertainties in the model parameters and in the model description appears to be important. In order to quantify the effect of each of these two types of uncertainty on the SWAN results, we plan to make a (relatively large) set of simulations in a Monte Carlo approach.

A classic dilemma of a Monte Carlo approach is the following. On the one hand we want to perform many simulations, since the accuracy of the results increases with the number of simulations. On the other hand, we are restricted by the amount of available computing time. The following aspects help to find a compromise:

- By using UATools (or a similar batch-run) to perform the Monte Carlo simulation on SWAN, the computation time required is merely 'waiting time'. Assuming some 40 minutes computation time per simulation, 36 simulations can be performed in 24 hours. The estimate required number of 190 simulations is then feasible within a week.
- Moreover, if we conclude that the accuracy of the result after one Monte Carlo run is not yet sufficient, we can perform an additional Monte Carlo run and combine the two to obtain a larger set. The convergence of the result typically evolves with the square root of the number of samples.

- Because the probability distributions of the uncertain parameters are not known in detail, the uncertainty in the SWAN results can only be quantified roughly. We will make estimates of the mean, the standard deviation and some non-extreme percentiles of the wave characteristics. These quantities can be determined based on a much smaller number of samples, compared to estimating extreme percentiles.

To quantify the uncertainty in the wave characteristics along the coast due to uncertainties in the model parameters, we estimate that a Monte Carlo analysis of a hundred to a few hundred samples will give satisfying results. With these simulations various types of statistical analyses can be performed to obtain information on, for example, correlations, relative sensitivities or conditional probabilities.

An alternative to the 'crude Monte Carlo' approach suggested is the so-called Quasi Monte Carlo (QMC) approach. This QMC method uses a more efficient way to obtain an ensemble for the uncertain parameters. We will consider using this method, or other forms of importance sampling.

Uncertain model description

Concerning the model description a more 'discrete' comparison is required, i.e. comparative simulations with and without a specific formula, or with different formulae describing the same physical process. Ideally, we combine the assessment of the parameters and the model descriptions, i.e. we consider the 'on' or 'off' switch for the model description as just another random variable in the Monte Carlo analysis.

Propagation of uncertainty to crest level

The SWAN uncertainty analysis will at least give an estimate of the uncertainty in the nearshore wave height and spectral period. This uncertainty will propagate into the HBC chain and lead to a contribution to the uncertainty in HBC and crest level.

In order to quantify this propagation, we will use the uncertainty information from the SWAN analysis to introduce a perturbation to the KustDB database, which contains results from SWAN calculations. To represent the uncertainties in the SWAN calculations, we apply a noise factor to the nearshore wave height and spectral period in the database. Starting from one reference KustDB, we generate an ensemble of databases, each with a different noise factor for wave height and period.

We apply one factor for wave height and one for wave period to each database in the ensemble, because these factors represent the uncertainty in the SWAN calculation, not in the individual wave parameters. Most likely, the uncertainty in the nearshore wave height and spectral period are correlated, so that the noise factor for wave height should be related to the factor for wave period. This correlation can be derived from the Monte Carlo analysis of the SWAN calculations. The same correlation is then applied to the database noise factors.

We estimate that an ensemble of 100 databases will be needed to represent the uncertainty in the SWAN calculations. This will not require significant computing time, as we intend to use a simple matlab script to generate an ensemble of databases from a single reference.

4.5 Monte Carlo 3: Uncertainty analysis of HBC

The third and final step in the HBC uncertainty analysis is to combine the ensemble of 100 sets of offshore storm events and the ensemble of 100 KustDB versions in a Monte Carlo run that randomly selects members from both ensembles and performs a Hydra-K calculation with the selected ensembles to produce a set of HBCs and the corresponding crest level. The result is an ensemble of crest levels that is based on many different combinations of storm events and KustDB versions. The variance of the crest level in this collection represents the total uncertainty in the HBC calculation.

An advantage of the stepwise approach to the uncertainty analysis is that we can easily determine the relative contributions of the two main sources of uncertainty: the marginal probability distributions of water level and wind speed and the SWAN calculations. If we exchange the ensemble of offshore storm events for the default unperturbed set of events we obtain a variance in crest levels that is caused by uncertainty in the KustDB (i.e. SWAN calculations) only. Likewise, if we use the reference KustDB and combine this with the ensemble of perturbed offshore storm events then we get a variance in crest level as a result of the uncertainty in the marginal distributions. This way, we can quantify the two main contributions to the total uncertainty in HBC, which is valuable information to identify efficient efforts to reduce the total uncertainty.

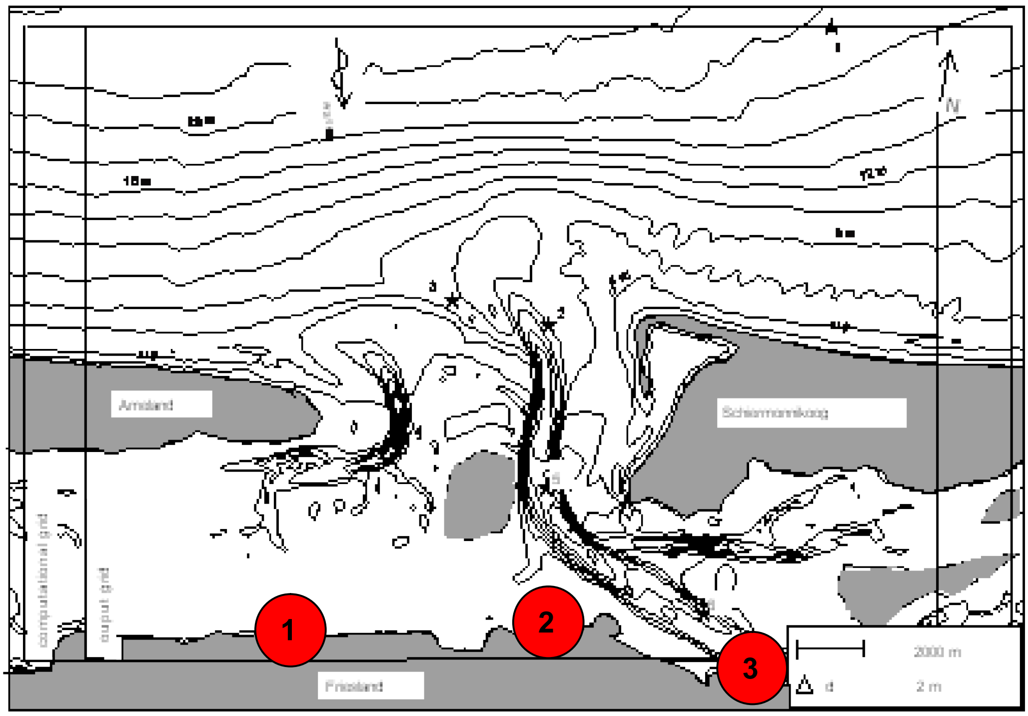

Figure 22 Locations for which the HBC will be calculated and the uncertainty analysis be done.

We propose to investigate the HBC uncertainty at three locations, indicated in Figure 22. Location nr 1 is largely shielded from the open sea by the island of Ameland. Location nr 2 is directly behind an inlet and is not shielded. This location will possibly receive swell waves. Location nr 3 is shielded by the island of Schiermonnikoog, but it is very close to a tidal channel, with strong currents and possible wave translation through the channel. We believe that these three locations capture most of the relevant phenomena in the Wadden Sea.

5 Summary and conclusions

5.1 Conclusion

We conclude that a stepwise Monte Carlo approach is most appropriate to investigate the uncertainty in Hydraulic Boundary Conditions (HBCs). Two separate Monte Carlo simulations will be performed for the two major sources of uncertainty in this calculation: the marginal exceedance probability functions of wind speed and water level on the one hand and the SWAN calculations on the other hand.

The propagation of uncertainty in the marginal probability functions to the water level and wind speed of an extreme storm event is analyzed using a matlab version of Hydra-K. The wind speed is randomized by applying a noise factor is $1+\varepsilon$, with ε drawn from a normal distribution with zero mean and a standard deviation of 0.2. The wind speeds of all the up-scaled storms are multiplied by this factor. The water level is randomized by applying a random shift, drawn from a normal distribution with zero mean and a standard deviation of 70 cm. This shift is added to the water levels of all uscaled storms.

The uncertainties in SWAN will be calculated using a special version of SWAN which is currently being developed. The test area will be the 'Friesche Zeegat' and the analysis will be done for severe storm conditions, comparable to the HBC.

The final step is to combine the two sources of uncertainty in a third Monte Carlo simulation and calculate how these propagate to an uncertainty in the HBCs. This uncertainty will be expressed as an uncertainty in the crest level, a single scalar quantity. In order to distinguish between the contribution of the two sources of uncertainty, we will perform separate runs with one of the sources of uncertainty switched 'off'. This will enable us to make estimates of the maximum achievable accuracy if either of the two sources of uncertainty is annihilated.

Finally, it is recommended to integrate the results of the current uncertainty analysis with the findings from two other studies:

- The investigation of the 'De Haan' method by WL | Delft Hydraulics focusses on the possible error associated with this statistical extrapolation method.
- The uncertainty in the failure calculations are investigated by GeoDelft within the SBW framework ('onzekerheidsanalyse faalmechanismen')

The total uncertainty in HBC should incorporate all contributions.

5.2 Planning for Phase 2

The basic uncertainty analyses will be done from September until November of 2007. The following steps will be taken:

1. Make a reference HBC calculation for the Friesche Zeegat (three locations).
    a. Prepare the SWAN model for Friesche Zeegat.
    b. Generate a KustDB for the Friesche Zeegat.

   c. Modify Hydra-K such that it calculates HBC for three nearshore locations in the Friesche Zeegat area.
   d. Calculate the HBC for these locations.
2. Do the SWAN uncertainty analysis, in a separate Monte Carlo simulation, using the UATools environment. We need to have the HBC (step 1) for this, because the SWAN uncertainty analysis is best done under critical (HBC) conditions.
3. Randomize the KustDB, based on the variance found in the SWAN uncertainty analysis
4. Randomize the storm event data in Hydra-K input.
5. Setup the overall HBC uncertainty analysis. Do three variations of Monte Carlo runs:
   a. randomized KustDB only.
   b. randomized storm events only.
   c. randomized kustDB and storm events.
6. Evaluate the results, do further analysis if necessary.
7. Write the report, QA.

The planned budget and time schedule for the activities mentioned above is as follows:

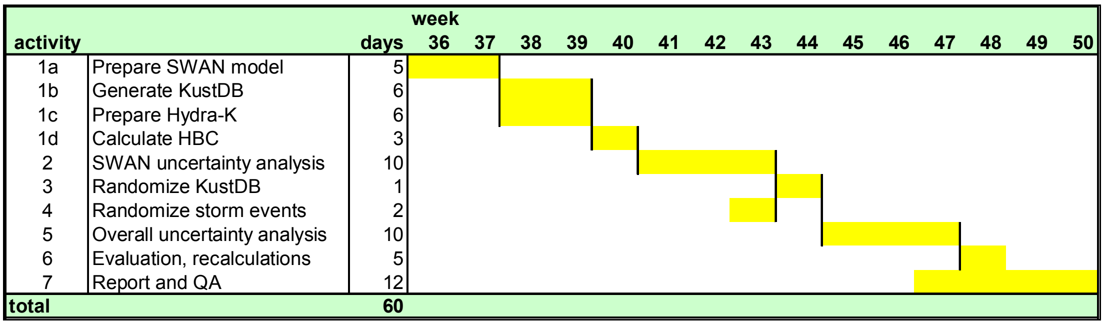

Figure 23 Schedule for phase 2. Vertical lines indicate dependencies.

Many of the activities depend on the results of other activities, as indicated by the vertical lines in Figure 23. For example, the SWAN uncertainty analysis (activity 2) can only start after the HBC for the locations in Friesche Zeegat are known (product of activity 1), because we choose to do the SWAN uncertainty analysis under critical (HBC) conditions. Also, the randomization of the KustDB (activity 3) must be done based on the results of the SWAN uncertainty analysis (activity 2). These and other dependencies pose the risk of delay of one activity to lead to delay of all other activities. Furthermore, in the schedule above, the final report is delivered at the very end of 2007. In case of a delay, the delivery of the final report will shift to the beginning of 2008.

We expect that the results from this study will give cause for some further research to investigate the various sources of uncertainty and their propagation in the HBC. The two main contributions to the total uncertainty can be further specified by analyzing their origin. For instance, the relative contributions of the SWAN parameters to the total uncertainty can be investigated. Moreover, the results of investigation of the 'De Haan' method and the failure mechanisms will become available by the end of 2007. We thus foresee substantial follow-up research in 2008.

6 References

Alkyon, 1999. SWAN met stroom, Alkyon Report A850.

Alkyon, 2003. Calibration of SWAN 40.20 for field cases Petten, Slotermeer, and Westerschelde, Alkyon Report A1168.

Alves, J.H.G.M., Banner, M.L., 2003. Performance of a saturation-based dissipation-rate source term in modelling the fetch-limited evolution of wind waves. J. Phys. Oceanogr. 33, 1274–1298.

Battjes, J. A., Janssen, J. P. F. M., 1978. Energy loss and set-up due to breaking of random waves. Proc. 16th Int. Conf. Coastal Eng., ASCE, 569-588.

Bouws, E. and G.J. Komen, 1983. On the balance between growth and dissipation in an extreme, depth-limited wind-sea in the southern North Sea, J. Phys. Oceanogr., 13, 1653-1658

Bretschneider, C. L., 1957. Hurricane design wave practices. ASCE, J. Waterw. Harbor Div., 83, 1238-1–1238-33. 1970: Forecasting Relations for Wave Generation. Look Lab Hawaii, 1, 31-34.

Brink, van den, H.W., Können, G.P., and Opsteegh,J.D., 2003. The reliability of extreme surge levels, estimated from observational records of order hundred years, Journal of Coastal Research, 19(2), 376-388.

Brink, van den, H.W., 2004. Extreme windopzetten en superstormen met behulp van numerieke klimaatmodellen. Eindrapport RKZ1006.

Bijl, W., Flather, R., de Ronde, J.G., Schmith, T., 1999. Changing storminess? An analysis of long-term sea level data sets, Climate Research, 11, 161–172.

Caires, Sofia, 2006a. Extreme wave statistics: methodology and applications to North Sea wave data. Activity 0.2 & 0.3 of SBW Wadden Sea, Opdrachtgever: Rijkswaterstaat RIKZ, WL report H4803.30.

Caires, Sofia, 2006b. Extreme wave statistics: confidence intervals. Activity 0.2 & 0.3 of SBW Wadden Sea, Opdrachtgever: Rijkswaterstaat RIKZ, WL report H4803.30.

Collins, J.I., 1972. Prediction of shallow water spectra, J. Geophys. Res., 77 (15), 2693-2707.

Dantzig, van, D., 1956. Economic decision problems for flood prevention. Econometrica, 24, 276-287.

Dillingh D, de Haan L, Helmers R, Können GP, van Marde J, 1993. De basispeilen langs de Nederlandse kust, Statisch onderzoek. Rijkswaterstaat, Tidal Water Division/National Institute for Coastal and Marine Management, The Hague, report no. DGW-93.023.

Eldeberky, Y., 1996. Nonlinear transformations of wave spectra in the nearshore zone. Ph.D Thesis, Fac. of Civil Engineering, Delft University of Technology, The Netherlands.

Geerse, C., Diermanse, F., Stijnen, J., 2006. Verbetering belastingmodellen. Rapportage fase II. HKV Lijn in Water rapport PR1161.

Groeneweg, J. and G.Ph. van Vledder, 2005. Tools for improving wave modelling and field measurements in shallow water. In Proc. of WAVES Conference, Madrid.

Groenewoud, P. and De Valk, 1999. C.F., DP Viewer version 3 Getting started, Argoss rapport.

De Haan, L. and Resnick, S.I., 1977. Limit theory for multivariate sample extremes. Z. Wahrscheinlichkeitstheorie, 40, 317-337.

Hasselmann, K., 1962. On the non-linear energy transfer in a gravity-wave spectrum. Part 1. General theory. J. Fluid Mech., 12 (4), 481-500.

Hasselmann, K., Barnett, T. P., Bouws, E., Carlson, H., Cartwright, D. E., Enke, K., Ewing, J. A., Gienapp, H., Hasselmann, D. E., Kruseman, P., Meerburg, A., Müller, O., Olbers, D. J., Richter, K., Sell, W., Walden, H., 1973. Measurement of wind-wave growth and swell decay during the Joint North Sea Wave Project (JONSWAP). Dtsch. Hydrogr. Z. Suppl., 12(A8).

Hasselmann, S., K. Hasselmann, J. A. Allender and T. P. Barnett, 1985. Computations and parameterizations of the nonlinear energy transfer in a gravity wave spectrum. Part 2: Parameterization of the nonlinear transfer for application in wave models. J. of Phys. Oceanogr., 15, 1378-1391.

HR2001, Hydraulische Randvoorwaarden 2001, voor het toetsen van primaire waterkeringen – Ministerie van Verkeer en Waterstaat: DGW, RIKZ, DWW, RIZA.

IPCC2007. Fourth Assessment Report (AR4) the Intergovernmental Panel on Climate Change (IPCC). Available from: www.ipcc.ch

Den Heijer, F., Vos, R.J., Diermanse, F.L.M., Groeneweg, J and Tonis, R., 2006. De veiligheid van de primaire waterkeringen in Nederland, Achtergrondrapport HR2006 voor de zee en estuaria, Rapport RIKZ/2006.029.

Holthuijsen, L.H., A. Herman, and N. Booij, 2003. Phase-decoupled refraction-diffraction for spectral wave models. Coastal Engineering, 49, 291-305.

Janssen, T. T., 2006. Nonlinear surface waves over topography. Ph.D Thesis, Fac. of Civil Engineering, Delft University of Technology, The Netherlands.

Kahma K.K. and C.J. Calkoen, 1992. Reconciling discrepancies in the observed growth of wind-generated waves. Journal of Physical Oceanography 22, 1389 – 1405.

Kahma, K. K., Calkoen, C. J., 1994. Growth curve observations. In: Dynamics and Modeling of Ocean Waves. Cambridge Univ. Press.

Kuik, A.J., Van Vledder, G.Ph and Holthuijsen, L.H., 1988. A method for the routine analysis of pitch-and-roll buoy wave data. J. Phys. Oceography, 18 (7), 1020-1034.

Madsen, O.S., Y.-K. Poon and H.C. Graber, 1988. Spectral wave attenuation by bottom friction: Theory. Proc. 21 th Int. Conf. Coastal Engineering, ASCE, 492-504

Marle, van J.,1999. Basis HYDRA-K. Meerdimensionale extreme-waardenstatistiek van belastingen en faalkansberekening. Rijksinstituut voor Kust en Zee (RIKZ), Den Haag.

Mathiesen, M., Hawkes, P., Martin, M.J., Thompson, E., Goda, Y, Mansard, E., Peltier E., and van Vledder, G., 1994. Recommended practice for extreme wave analysis. J. Hydraulic Res., IAHR, 32 (6), 803-814.

Ruessink, B.G., D.J.R. Walstra and H.N. Southgate, 2003. Calibration and verification of a parametric wave model on barred beaches. Coastal Engineering, 48, 139-149.

Rijkoort, P.J., 1983. A compound Weibull model for the description of surface wind velocity distributions. Scientific Report, WR 83-13, Royal Netherlands Meteorological Institute (KNMI).

Shemdin, O., K. Hasselmann, S.V. Hsiao and K. Herterich, 1977. Nonlinear and linear bottom interaction effects in shallow water. In: Turbulent fluxes through the sea surface, wave dynamics, and prediction. Ed. A. Favre. New York: Plenum Press.

Sigmond et al, 2006. Zachtere winters door klimaatveranderingen op grote hoogte. KNMI report, available at: www.kennislink.nl/web/show?id=145681

Snyder, R. L., Dobson, F. W., Elliot, J. A., Long, R. B., 1981. Array measurements of atmospheric pressure fluctuations above surface gravity waves. J. Fluid Mech., 102, 1-59.

Stijnen, J.W., Duits, M.T. and Thonus, B.I., 2005. Hydra-K voor de HR2006, HKV Report for Rijkswaterstaat RIKZ.

Stijnen, J.W., Duits, M.T. and Thonus, B.I., 2005b. Diepwaterrandvoorwaarden (ELD, EUR, YM6, SCW en SON), HKV Report for Rijkswaterstaat RIKZ.

Smits, A. 2001, Analysis of the Rijkoort-Weibull model. KNMI report HYDRA project. Available from http://www.knmi.nl/samenw/hydra.

Smits, A., Klein Tank, A.M.G. and Können, G.P., 2002, Trends in storminess over the Netherlands, 1962-2002. KNMI report HYDRA project. Available from http://www.knmi.nl/samenw/hydra.

SWAN-team, the, 2007. SWAN USER MANUAL. SWAN Cycle III version 40.51A. Delft University of Technology. Available at http://vlm089.citg.tudelft.nl/swan/index.htm

TAW, 1998. Grondslagen voor waterkeren, Technische Adviescommissie Waterkeren, Technical Report, available at www.tawinfo.nl.

Timmerman, H.,1977. Meteorological effects on tidal heights in the North Sea. Staatsdrukkerij, 's Gravenhage.

Verkaik, J. W., Smits, A. and Ettema, J., 2003. Naar een nieuwe extreme waardenstatistiek van de wind in Nederland, HYDRA project, faserapport 16, KNMI.

Verkaik, J. W., 2001. Documentatie Windmetingen In Nederland Koninklijk Nederlands Meteorologisch Instituut, Klimatologische Dienst (unpublished report).

Voortman, H.G, 2002, Risk-based design of large-scale flood defence systems, Phd-thesis Delft University of Technology, Fac. of Civil Engineering.

VTV 2004, De veiligheid van de primaire waterkeringen in Nederland. Voorschrift Toetsen op veiligheid voor de tweede toetsronde 2001-2006 (VTV). Publicatie van Ministerie van Verkeer en Waterstaat.

De Waal, J.P. 2003, Windmodellering voor bepaling waterstanden en golven. Een analyse van bouwstenen. RIZA werkdocument 2003.118x.

Van der Westhuysen, A.J., Zijlema, M. and Battjes, J.A., 2007. Nonlinear saturation-based whitecapping dissipation in SWAN for deep and shallow water, Coastal Engineering 54 (2007) 151–170.

Wet op de Waterkering, 1995, Wet van 21 december 1995, houdende algemene regels ter verzekering van de beveiliging door waterkeringen tegen overstromingen door het buitenwater en regeling van enkele daarmee verband houdende aangelegenheden, available from: http://wetten.overheid.nl/

WL, 2002. The ONR Testbed for coastal and oceanic wave models, Version 2.0. WL | Delft Hydraulics Report H3627.

WL, 2005. Diermanse, F.L.M., Weerts, A.H., Wenneker, I. and Groeneweg, J., 2005. Analyse golfstatistiek op relatief diep water. Studie ten behoeve van het afleiden van betrouwbaarheidsintervallen en fysische bovengrenzen van de golfhoogte en golfperiode. WL | Delft Hydraulics Report Q3966.

WL, 2006a. Storm Hindcasts Norderneyer Seegat and Amelander Zeegat. WL | Delft Hydraulics Report H4803.11.

WL, 2006b. Calibration tool for SWAN. Activity 8.1 & 8.2 of SBW project Waddenzee. Part 1: Analysis of requirements. WL | Delft Hydraulics Report X0346.

WL, 2007a. Van der Klis, H. and Diermanse, F.L.M., Uncertainties in the Hydraulic Boundary Conditions of the Wadden Sea. WL | Delft Hydraulics Report Q4267.20

WL, 2007b. Van der Westhuysen, A.J., Reducing the computational time of SWAN by dynamic deactivation of grid points. WL | Delft Hydraulics Report H4918.37.

Young, I.R., 1999. Wind generated ocean waves. Elsevier Ocean Engineering Book Series. Volume 2. Oxford: Elsevier.